Dominik WINKLER

STIFFNESS BEHAVIOR OF DOUBLE-SHEAR WOOD-STEEL SHEET CONNECTIONS

MASTERARBEIT

eingereicht an der

LEOPOLD-FRANZENS-UNIVERSITÄT INNSBRUCK
FAKULTÄT FÜR TECHNISCHE WISSENSCHAFTEN

Zur Erlangung des akademischen Grades

DIPLOM-INGENIEUR

Beurteiler:

Univ. Prof. Dr. Michael Flach

Institut für Konstruktion und Materialwissenschaften

Arbeitsbereich Holzbau

Innsbruck, September 2016

Betreuer: Univ.-Prof. DDipl.-Ing. , Michael Flach
LEOPOLD-FRANZENS-UNIVERSITÄT INNSBRUCK,
Institut für Konstruktion und Materialwissenschaften,
Arbeitsbereich Holzbau

Widmung

Diese Arbeit widme ich meiner Mutter *Lageder Reinhilde,* für alles was sie für unsere Familie geleistet hat.

Donkschian Mama.

Acknowledgement

Austrian Marshall Plan Foundation for the financial support.

Rotho Blaas S.R.L. for the donation and shipment of the examined self-tapping bolts.

Nordic Structures for the donation of the glulam beams.

Alexander C. Schreyer, Dipl.-Ing. and Peggi L. Clouston, Ph.D. for all their support and for the great opportunity to write this thesis at the department of Building and Construction Technology at the University of Massachusetts Amherst.

Michael Flach, Univ.-Prof. DDipl.-Ing. for setting up the initial contact and for the ongoing support.

Roland Maderebner, Dipl.-Ing. for the idea to this thesis and for the ongoing support.

L. Carl Fiocchi, Ph.D. for the enormous help editing this thesis and especially for all the nice conversations, life lessons and never the last all the laughter and happiness. Thanks.

Abstract

Der moderne Holzbau steht und fällt mit der Verbindungstechnik. Der Aspekt der Tragfähigkeit wurde in der Vergangenheit ausführlich betrachtet, und Formelwerke zur Berechnung erstellt. Aufgrund der Vielzahl an Verbindungsmitteln und der Variation der Holzeigenschaften ist es jedoch immer noch schwierig eine Aussage über die Steifigkeit zu machen. Zum Zweck eines besseren Verständnisses für die Berechnung der Steifigkeit von Verbindungen mit selbstbohrenden Stabdübeln wurden die amerikanische sowie die europäische Holzbaunorm miteinander verglichen. In einem ersten Testprogramm wurden Daten für das Verhalten der einzelnen Stabdübel erhoben. Anhand dieser Daten wurde dann versucht, die Steifigkeit einer Verbindung mit einer Gruppe von Verbindungsmitteln zu berechnen. Die so berechneten Steifigkeiten wurden dann mit den Werten aus einer zweiten Testreihe verglichen. Als Ergebnis wurden zwei Faktoren bestimmt, welche eine genaue Berechnung / Simulation der Verbindungssteifigkeit ermöglichen.

Abstract

The modern timber construction stands and falls with the connection-technique. The aspect of load bearing capacity was extensively examined in the past and calculation-formulas for this purpose have been developed. Caused by the huge number of different connectors and the variation in the properties of the timber, the prediction of a connection's stiffness is still difficult. For the purpose of a better understanding for the calculation of a connections stiffness, wherein self-tapping bolts are used, both, the American and the European code were compared. In a first testing program, data has been gathered for the behavior of single fasteners. Based on this data, the stiffness of a connection with a group of fasteners was predicted. Comparing the calculated values with those gathered in a second testing program, two factors were determined that allow a better calculation / simulation for the connections stiffness.

Table of Contents

List of Figures

List of Tables

List of Equations

List of abbreviations

CLT	Cross Laminated Timber
e.g.	Exempli Gratia
FEM	Finite Element Method
Glulam	Glued Laminated Timber
i.e.	Id Est
Lamboo	Laminated Bamboo
LVDT	Linear Variable Differential Transformer
LVL	Laminated Veneer Lumber
m.c.	Moisture content
No.	Number

1 Introduction

Timber construction has a long tradition, for centuries it was a principle building material used throughout the world. Over the decades, many different connection types have been developed and improved upon. From simple wood-to-wood connections, over nailed connections to the modern bolted connections (Figure 1-1), to mention some of the techniques. Since wood is a natural material and due to the fact that it experienced the forces of both "wind and weather" during its growth, each specimen exhibits idiosyncratic characteristics. Timber is an anisotropic material, which means that its properties vary with the direction of its fibers. These inconsistencies create problems and make it more difficult to design with timber; especially when compared to commonly used manmade building materials, e.g. steel or concrete. When focus is targeted at structural stiffness, this variation in timber characteristics presents obstacles.

Figure 1-1: Modern bolt connection with self-tapping bolts and glulam beams [1]

In the past, substantial research has been done referencing nails, screws, and bolts. Most of which was involved in calculating the load carrying capacity and prediction of the failure mode. A large part of the research was also done on engineered timber materials, e.g. laminated veneer lumber (LVL) and cross-laminated timber (CLT) [2].

Designing connections means calculating the maximum strength, as well as analyzing the behaviors under load. Typically, the connections should be designed as stiff as possible, while simultaneously demonstrating a distinct ductile behavior. Therefore, it is of importance to examine the load-deformation curves and to analyze and understand the characteristics (Figure 1-2 and Figure 1-3).

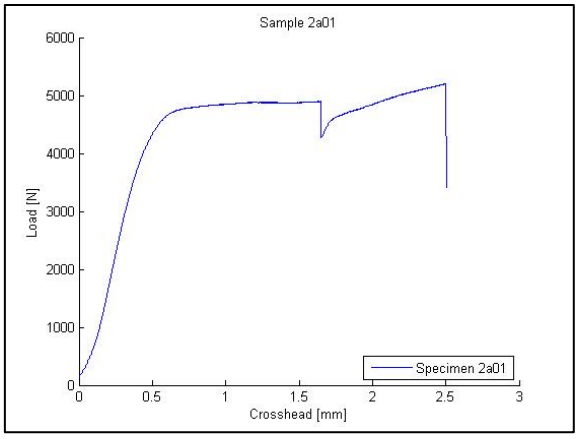

Figure 1-2: Typical load-displacement curve - load parallel to grain

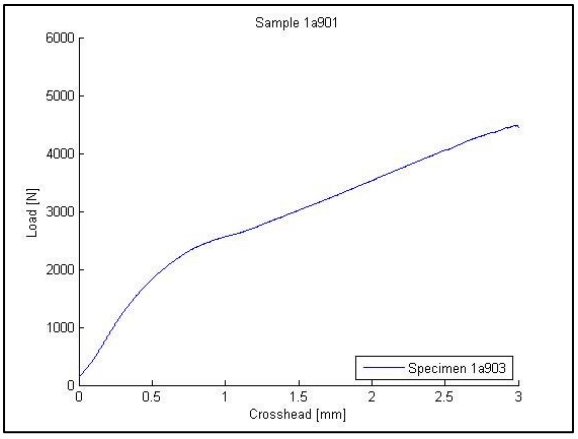

Figure 1-3: Typical load-displacement curve - loaded perpendicular to grain

Based on the knowledge gathered from the analysis, the connection can then be designed to force failure at the point where the connector demonstrates the optimal ductile failure. Failures associated with low ductility, i.e. brittleness have to be avoided because of the suddenness of the failures that leaves no opportunity for intervention or emergency evacuation.

This thesis' intent is to examine the stiffness of connections in structural timber design. In order to achieve the desired goals, a comprehensive literature research was undertaken referencing both the European and American Standards. Both testing protocols were adhered to while executing the computational simulations.

2 Basics

Bolted connections, in general, are made of two or more structural components connected with a specified number of bolts. The structural elements are typically two or more wooden beams connected to each other or to metal plates. The connectors transfer the loads from one part of the structure to another. In order to design the connection, to meet the requirements of an actual situation, can involve many variables; for example, the diameter or number of the bolts. Figure 2-1 shows a 15-bolt connection joining a glulam beam to a joint, in this particular case with six shear planes (two at each metal plate).

Figure 2-1: Example of bolted connection with multiple layers of steel

The majority of the research in the past was done on the load carrying capacity of these connections. Johansen in 1949 [3] did an exceptional research, attempting to establish formulas to calculate the maximum load for one single bolt. His work was based on a double shear connection with a total of four different possible failure modes (Figure 2-2 and Figure 2-3).

Meyer in 1955 [4] extended Johansen's *Yield Theory* to single-shear assemblies with different material properties; those equations are the basis of most of the present-day building codes.

However for the calculation of a structure it is also very important to know how the loads are distributed and conducted to the ground, especially in statically indeterminate structures. For this matter the stiffness of the single parts and the connections in between play a key role. Particularly the calculation of a connections stiffness is challenging due to the different mechanisms that are involved.

For the stiffness of a connection, the load-slip curves (Figure 1-2 and Figure 1-3) of the single fastener are important. They describe how much displacement will appear under a certain force. The procedure to obtain the load-slip curves as well as the maximum embedment strength is described in ÖNORM EN 383 [5] respectively in ASTM D 5764 [6].

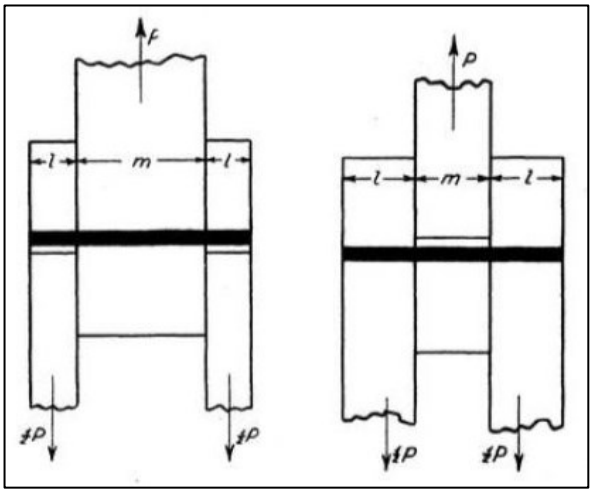

Figure 2-2: Failure modes 1 and 2 [3]

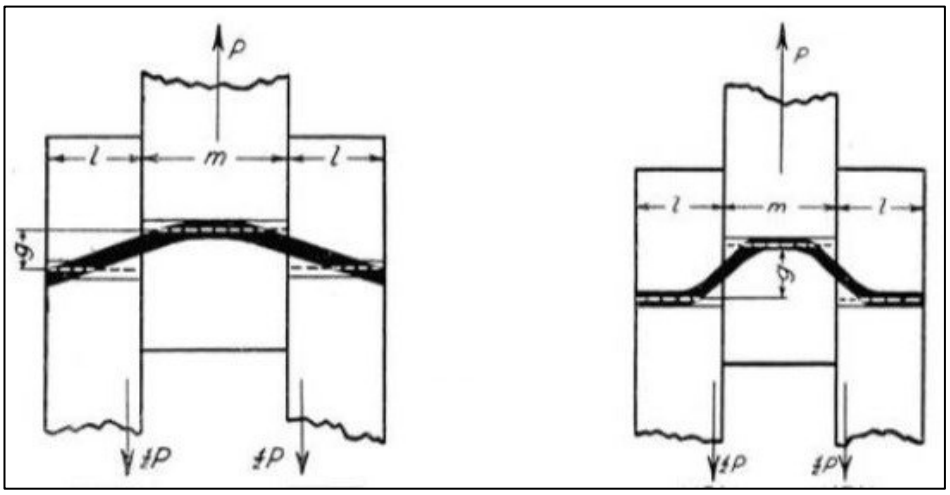

Figure 2-3: Failure modes 3 and 4 [3]

As mentioned most connections are idiosyncratic, tailor-made for the static system they are used in. It is not possible to provide general formulas covering all the possible scenarios. Every connection must be examined separately, taking into account the individual stiffness of each component of the whole. In order to simplify the calculation of a connection's stiffness, the European code (ÖNORM B 1995-1-1) provides formulas that allow estimating the slip modulus at yield load (K_{ser}), and at ultimate load ($K_u = 2/3 * K_{ser}$). The formulas for K_{ser} are presented in Table 2-1 and represent values for one shear-plane of a fastener, connecting two timber parts. For the case of a timber to steel or timber to concrete connection these K_{ser} values are multiplied by a factor 2. This takes into account that steel and concrete are much stiffer than timber; an insignificant amount of deformation will occur in the steel or concrete component, which leads to half of the deformation. This respectively doubles the stiffness that a wood-to-wood connection would exhibit.

Table 2-1: Slip modulus K_{ser} according to ÖNORM B 1995-1-1 [7]

Fastener type	**K_{ser}**
Dowels Bolts with or without clearance[a] Screws Nails (with pre-drilling)	$\rho_m^{1.5}d/23$
Nails (without pre-drilling)	$\rho_m^{1.5}d^{0.8}/30$
Staples	$\rho_m^{1.5}d^{0.8}/80$
Split-ring connectors type A according to EN 912 Shear-plate connectors type B according to EN 912	$\rho_m d_c/2$
Toothed-plate connectors: − Connectors types C1 to C9 according to EN 912 − Connectors type C10 and C11 according to EN 912	 $1.5\rho_m d_c/4$ $\rho_m d_c/2$
[a] The clearance should be added separately to the deformation.	

For deflection calculations at yield- respectively ultimate load, this linear elastic approach with K_{ser} may be an easy and sufficiently exact option, however the inelastic information is lost. Earthquake calculations, for example, need more detailed stiffness information in order to examine energy dissipation in the system. Garvic [8] supposed a more detailed approximation with a piecewise linear approach (Figure 2-4), that describes the elastic branch (k_{el}), the first plastic (hardening) branch (k_{pl}), and the second plastic (softening) branch (k_{p2}).

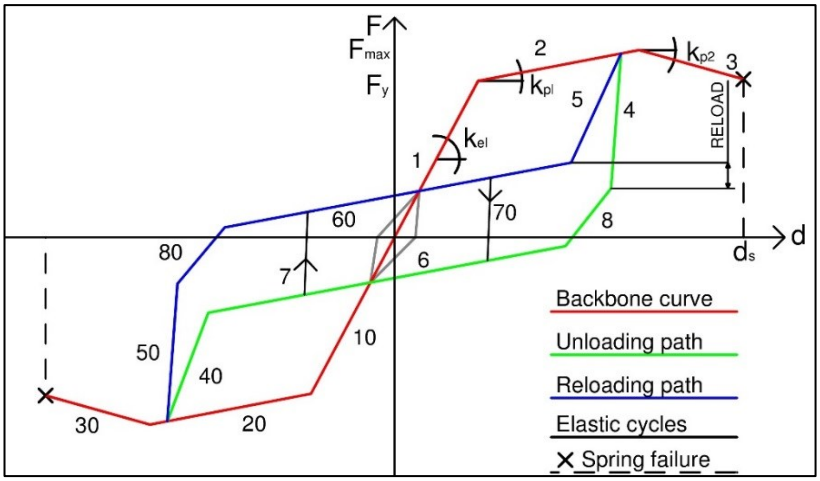

Figure 2-4: Piecewise linear approach [8]

Taking such idealized curves as basis, computational models can be established. Depending on the requirements, finite element method (FEM) software such as ABAQUS or ANSYS or even common static programs for civil engineering like can be used to calculate exact connection behavior. Hochreiner [9] describes the integration and calculation of connection slip in commercial static software and gives advice instructing how to create accurate models.

2.1 State of the art

The building codes of different countries can be seen as the state of the art. Periodically new research is undertaken, which results in new findings, which increase assurances relating to durability and safety over lifetime of a construction project. While building codes vary from country to country, this thesis focuses on the European "Eurocode", which is represented by the Austrian "ÖNORM B 1995-1-1" [7]; and the American "ANSI/AWC NDS" [10].

2.1.1 Eurocode

The Eurocode is the common code of the European Union. It is elaborated by the European Committee of Standardization (CEN) and represents the harmonized standards for all 33 CEN Members.

Timber design is described in the ÖNORM B 1995-1-1. The determination of embedment strengths and bending moments of fasteners the code refers to EN 383 [5] and EN 409 [11] and EN 1380 [12]. In Chapter 2.2, the EN 383, which is describing the testing procedure for the embedment strength, is compared to the American counterpart ASTM D 5764.

2.1.2 ANSI

In the United States, the American National Standards Institute (ANSI) represents the counterpart to the European CEN.

The ANSI accredited the American Wood Council (AWC) as the standard developing organization in timber engineering. The current standard for timber construction in the U.S. is the ANSI/AWC NDS-2015.

2.2 Comparison of testing codes EN 383 and ASTM D 5764

The EN 383 as well as the ASTM D 5764 aims to provide the maximum bearing strength of dowel type fasteners such as bolts, dowels, and nails in timber or timber based products. To achieve this goal, the codes describe a standardized procedure with regulations for the key elements of the test. The codes describe how to produce and season the timber specimen, how to place them in the testing rig, how to apply the load, and most importantly they specify the variables subject to measurement.

2.2.1 Comparison of the setup

Based on the diameter of the dowel, the dimensions of the wood specimen are limited. The two principle reasons for these limitations are:

- Eliminating bending of the dowel
- Eliminating the risk of splitting at the loaded end

Both codes apply a certain ratio of dowel diameters for the specimen dimensions (Table 2-2); in addition, ASTM D 5764 provides absolute minimum dimensions, which applies to dowel diameters less than 12.5 mm (*4.92 inch*).

The required dimensions for the specimens examined in this thesis are shown in Table 4-1. Note: larger minimum dimensions are generally found in EN 383 than in its American counterpart.

The Specimen, in both cases, is a prismatic body with parallel fiber direction. To avoid the effects of manufacturing failures and natural defects, which might be notch holes or parts with cross grain, the specimen should be from a timber with very clear and straight grain. Exceptions to this rule are allowed, if the influence of these defects is part of the research.

Before testing, the wood must be conditioned in a controlled climate at 20 $\pm$ 2 °C with relative humidity of 65 $\pm$5 % as specified by EN 383. ASTM D 5764 does not require specific conditions; the specimen should be seasoned relative to the scope of the testing program.

A general difference between the two protocols is that EN 383 only describes full-hole tests, whereas ASTM D 5764 generally is based on half-hole tests; a full-hole test setup is only intended with specimens that tend to split. Testing a full-hole setup has the disadvantage that the applied forces tend to bend the bolt (Figure 2-5), whereas on a half-hole setup the forces are applied directly in the area where the bolt is bared by the timber specimen. This means that results from half-hole tests are by nature free of effects deriving from bending of the bolt. Nevertheless full hole tests are more accurate because tensions in real world applications are distributed all around the hole.

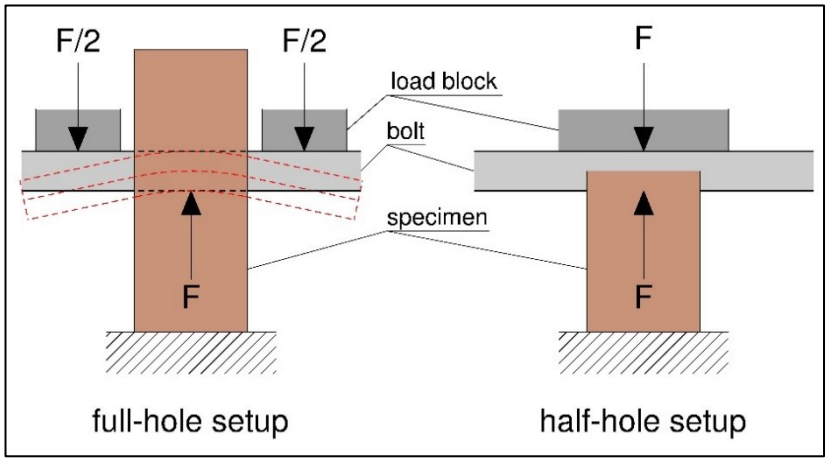

Figure 2-5: Deformation of loaded bolt

Table 2-2: Specimen dimension requirements[1]

		EN 383		ASTM D 5764	
		Min	**Max**	**Min**	**Max**
Load Parallel to Grain	**Loaded End**	7d	/	the larger of: 50 mm (*2 inch*) or 4d	/
	Unloaded End	7d	/	the larger of: 25 mm (*1 inch*) or 2d	/
	Width	10d	/	the larger of: 50 mm (*2 inch*) or 4d	/
	Thickness	1.5d	4d	the smaller of: 38 mm (*1 1/2 inch*) or 2d	/
Load Perpendicular to Grain	**Loaded End**	5d	/	the larger of: 50 mm (*2 inch*) or 4d	/
	Unloaded End	5d	/	the larger of: 25 mm (*1 inch*) or 2d	/
	Width	40d	/	the larger of: 50 mm (*2 inch*) or 4d	/
	Thickness	1.5d	4d	the smaller of: 38 mm (*1 1/2 inch*) or 2d	/

Additional significant differences between the two codes can be observed in the measurement of displacements as well as in the application of load.

[1]EN 383 provides different dimensions for Nails and timber products with more than one fiber direction; these are not shown in this table

EN 383:	ASTM D 5764:
Displacement measuring	
The measurement points are located at a defined distance at the height of the hole (Figure 2-6). Measurement should be taken at both sides of the hole. The actual displacement equals the average of both measurements. In theory this measuring method is very accurate, and represents the actual displacement of the bolt referred to the initial position in the wood. Especially with smaller specimen and bolt dimensions it gets harder to set the measurement devices the right way.	The measured distance is the displacement between movable - and stationary crosshead. The disadvantage of this method is the fact, that the measured deformation is affected by the stiffness of the wood specimen (indicated by the blue arrow in Figure 2-7). Differences to EN 383 are small but noticeable.
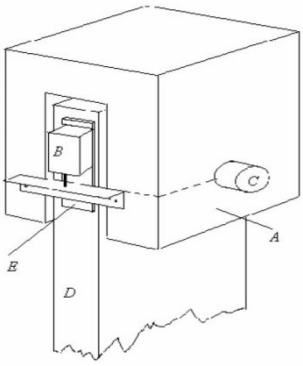	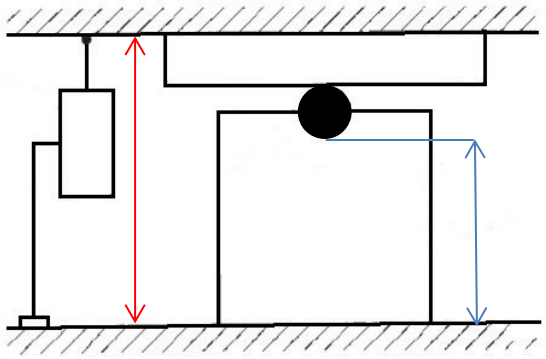
Figure 2-6: Test setup EN 383 [5]	*Figure 2-7: Test setup ASTM D 5764 [6]*
Loading	
Figure 2-8 shows the load application over test-time. It is characterized by a first loading to 0.4 times the estimated maximal load F_{est}, maintaining it at this level for 30 seconds, and then reducing it to 0.1 times F_{est}. After another 30 seconds, the load is increased until failure of the specimen or until a maximum displacement of 5 mm (*0.197 inch*) is reached. The testing speed shall be chosen in a manner that the	Load is applied at a constant speed from the beginning. The test ends at rupture of the wood or at a crosshead displacement of 0.5 times the bolt diameter d. An initial loading and unloading cycle is not provided. The maximum load shall be reached in 1 to 10 minutes.

last loading cycle until F_{est} takes (300 ± 120) seconds.

The reason for this first loading-unloading cycle is to simulate the real world situation, where a certain time passes from the installation of the bolt until the final loads are applied. In this time the bolt in a manner of speaking "settles" in the hole.

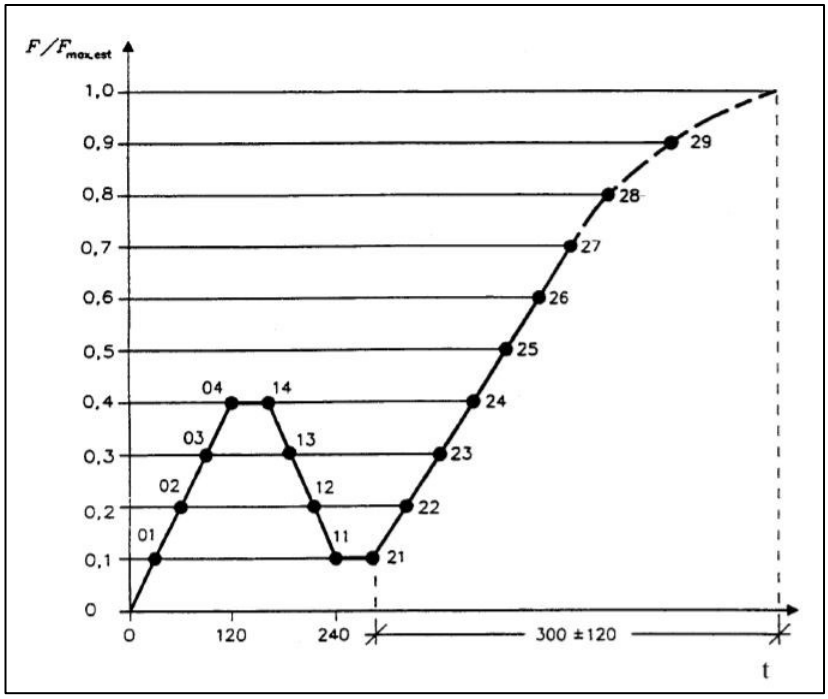

Figure 2-8: EN 383 loading cycle [5]

2.2.2 Interpretation of results

The results of these tests are load-displacement-curves, such as seen in Figure 1-2 and Figure 1-3. An initial almost straight line with a steep slope describes the elastic behavior of the material. The first line is followed by a second straight line with a less severe slope. The second line describes the plastic behavior of the material.

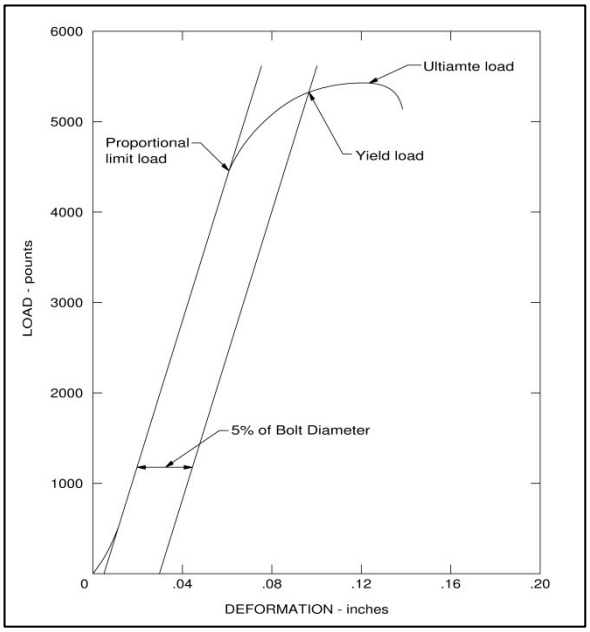

Figure 2-9: ASTM D 5764 yield load [6]

Although both codes attempt to establish a value for the identical material-property, the way that they interpret these curves is different. The load in the EN 383 corresponds to the ultimate / maximum load. ASTM D 5764 alternatively, fits a straight line to the first slope and offsets it by 5% of the bolt diameter, to the right. The intersecting point between this line and the load–displacement curve results in the yield load (Figure 2-9).

The bearing strength, f_h, is then calculated by dividing the preserved load L by the thickness t of the specimen and the bolt diameter d.

$$f_h = \frac{L}{t * d} \qquad 2.1$$

The results of the tests performed in Chapter 4 show, that for the tests where the load is applied parallel to the grain, the resulting bearing strength demonstrates a strong correlation between the two codes. However the results provided by the different codes differ in tests perpendicular to the grain. Caused by the steeper slope of the plastic branch in the load-deformation curves and the different approach to determine the controlling load the difference in bearing-strength is significant.

Due to the cyclic loading in EN383 it is possible to calculate different stiffness-moduli based on the resulting load-displacement curve (Figure 2-10).

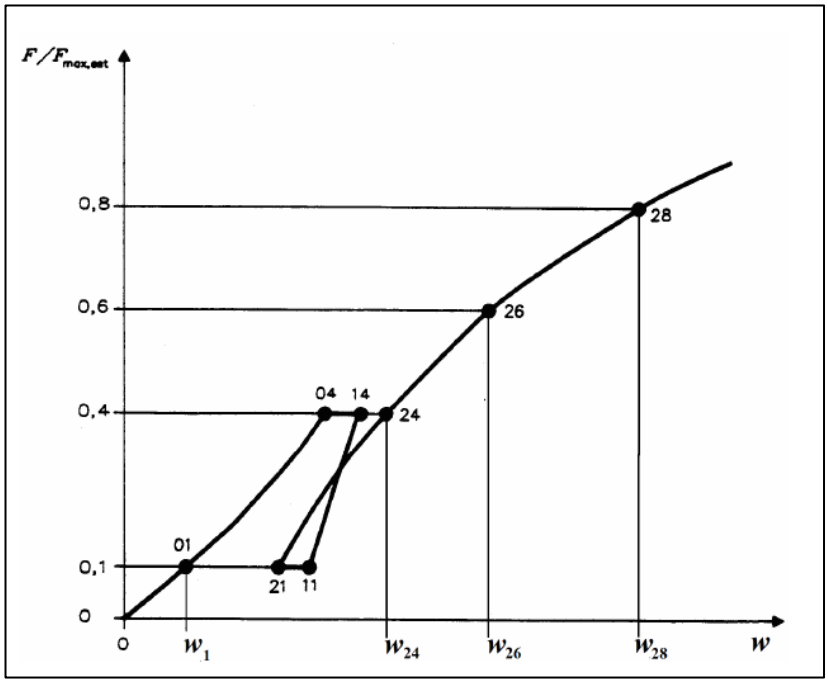

Figure 2-10: Idealized load-displacement curve according to EN383

Initial embedment modulus:

$$K_i = \frac{0.4 * f_{h,est}}{w_i} \qquad 2.2$$

$$w_i = w_{04} \qquad 2.3$$

Elastic embedment-modulus:

$$K_e = \frac{0.4 * f_{h,est}}{w_e} \qquad 2.4$$

$$w_e = \frac{2}{3}(w_{14} + w_{24} - w_{11} - w_{21}) \qquad 2.5$$

Embedment-modulus:

$$K_s = \frac{0.4 * f_{h,est}}{w_{i,mod}} \qquad 2.6$$

$$w_{i,mod} = \frac{3}{4}(w_{04} - w_{01}) \qquad 2.7$$

3 The connection

The connection examined in this thesis is a typical bolted double shear steel to timber connection loaded with shear and moment. The bolts (Figure 3-1) used within the connection are self-tapping, meaning that there is no need to predrill a hole before inserting the bolt. From the perspective of load carrying, there should not be a difference between self-tapping bolts and traditional bolts; however, it is expected that the stiffness of the connection without the predrilled hole is greater.

3.1 Materials and equipment

The Bolts used in this thesis were "Rothoblaas WS-T-7x133" provided by Rothoblaas, an Italian manufacturer. The bolts are made of carbon steel, coated with galvanic zinc. A cutting tool is attached to the tip of the bolt, to allow for a fast installation with precise fit into the connection. They have a nominal diameter of 7 mm (*0.276 inch*) and a nominal length of 133 mm (*5.24 inch*).

According to the manufacturer's datasheet, the minimum yield strength, $f_{yk,}$ is 1'000 MPa and the characteristic yield moment is 31.93 kNm (*23'550.35 lb.ft.*).

Figure 3-1: Rothoblaas WS – self-tapping bolt [1]

The wood specimens for single hole embedment tests were of three different materials.

- White ash
- Lamboo, (laminated bamboo)
- Glulam, (Black Spruce in the form of Glued-laminated-timber)

White Ash (Fraxinus Americana), also known as American Ash, is a hard wood, widely occurring in northeast America (Figure 3-2).

Its density is 670 kg/m^3 (*0.683 specific gravity*[2]), with a moisture content of 12%. Due to its high strength and shock resistance, it is a commonly used wood for tool handles, baseball bats, and flooring. Research is being done to use White Ash in construction; possible applications are in the production of glulam or CLT. The specimens, used in this thesis were made of clear boards of White Ash (non-engineered).

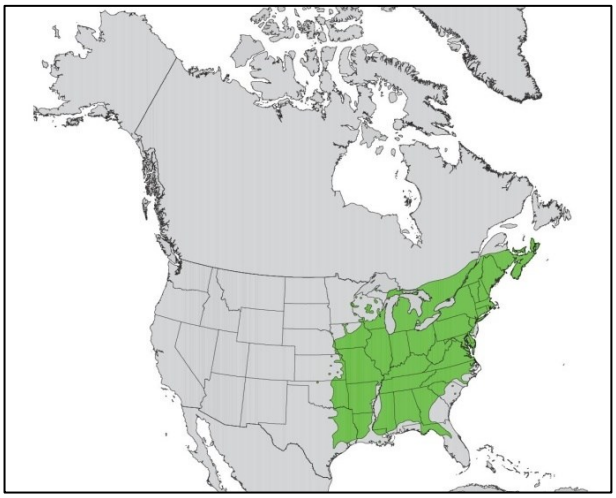

Figure 3-2: Distribution of White Ash [13]

Lamboo is an engineered product made from bamboo. An engineered product is one where the raw material is sorted and processed; only clear strands of bamboo are used. These high quality selections of bamboo are then glued together to create large structural beams for use in construction. The density of the finished Lamboo is 673 kg/m^3 (*0.686 []*), which is comparable to White Ash. Even though the bamboo was originally a grass and not a tree, it is compared to timber products in this thesis for the following reasons:

- Lamboo with its fiber structure is an anisotropic material such as timber; its behavior under stress should therefore be similar.
- It is competing against timber products in construction.

[2] Specific gravity is a value that compares the gravity of a material to the gravity of water; it is therefore unit-less.

$$SG = \frac{\rho_{sample}}{\rho_{H2O}}$$

Black Spruce (picea marinara) as opposed to the White Ash and Lamboo is a soft wood with a density of approximately 410 kg/m^3 (*0.418 []*). It grows almost exclusively in Canada and Alaska (Figure 3-3). Due to the harsh climate of those regions, the Black Spruce tends to be a smaller tree and therefore historically of less value to the construction industry. Today, however, with the development of engineered timber products, it is possible to use these smaller diameter trees to produce i.e. glulam beams (Figure 2-1).

Figure 3-3: Distribution of black spruce [14]

The Black Spruce used in this thesis was provided by Nordic a Canadian supplier. All specimens were made from 3.05 m (*10 feet*) long 137 mm (*5 3/8 inch*) by 267 mm (*10 1/2 inch*) glulam beams stress grade 24F-ES/NPG.

Figure 3-4 shows the cross-section of the glulam beam. By observing the diameter of the yearly growth rings, a small diameter of the trees can be adumbrated. In response to that smaller diameter, the individual rectangular elements are constrained to a thickness of 22.85 mm (*0.9 inch*) and a width of 45.72 mm (*1.8 inch*).

Figure 3-4: Structure of glulam beam

Table 3-1: Specific strength and design properties according to Nordic [15]

Bending about X-X or Y-Y axis	
Bending moment (F_b)	30.7 MPa
Longitudinal shear (F_v)	2.5 MPa
Compression perp. to grain (F_{cp})	7.5 MPa
Shear-free modulus of elasticity (E)	13’100 MPa
Apparent modulus of elasticity ($E_{app.}$)	12’400 MPa
Axially loaded	
Compression parallel to grain (F_c)	33.0 MPa
Tension parallel to grain (F_t)	20.4 MPa
Tension perp. to grain (F_{tp})	0.51 MPa
Modulus of elasticity (E_a)	13’100 MPa
Connections design	
Mean relative density (G)	0.47 []
Characteristic density (ρ_k)	430 kg/m^3
Density (for member weight) (ρ)	560 kg/m^3

All tests have been performed on a **MTS 30/G** testing machine, manufactured by MTS Systems Corporation, outfitted with computational data fetching. It is a strain-controlled load test machine with a maximum load of 150 kN (*30'000 lb.*).

Load cell: The load cell is also produced by MTS, it is capable of measuring loads up to 150 kN (*30'000 lb.*). The most recent documented calibration took place in December 2010, where a maximal tolerance of +/- 0.19 % of applied force according to ASTM E4-10 method was noticed. This tolerance is within the machines specific tolerance of 1 %.

Table 3-2: MTS 30/G

	kN	**lb.**
Applicable force	150	30
Max. Tolerance	+/- 1 %	
Tolerance of last calibration (20 Dec. 2010)	+/- 0.19 %	

The moisture content was measured with a **Delmhorst RMD-3** moisture meter manufactured by Delmhorst. It provides moisture content readings from 5 % to 60 %[3] with a resolution of 0.1 %. In addition, it measures the room temperature and the output's statistical values. With the integrated contact pins, the wood is penetrated 7.9 mm (*5/16 inch*) to measure the moisture content of the specimen.

The moisture content was also calculated over the weight at test time and its "oven-dry" dry weight according to the EN 322 [16] procedure.

LVDT: The **LVDT**s (linear variable differential transformer) used to measure the deflections were manufactured by Novotechik and have the following specifications:

Table 3-3: Specifications of LVDTs

No.	**LVDT**	**mechanical measuring range**	**electrical measuring range**	**linearity [%]**
1	T0025	30 mm (*1.18 inch*)	25 mm (*0.98 inch*)	± 0.2
2+3	T0050	55 mm (*2.17 inch*)	50 mm (*1.97 inch*)	± 0.15
4	TR25	30 mm (*1.18 inch*)	25 mm (*0.98 inch*)	± 0.2

LVDT No. 4 was connected to the input at the testing machine and the retrieved data is directly incorporated in the MTS software. LVDTs No. 1 - 3 were purchased new and did

[3] The device is calibrated for Douglas Fir, by determining the examined wood species, values are corrected automatically.

not have fitting connectors, for that reason a USB data logger that allows connecting the raw wires was used, in order to retrieve the data.

Power was provided by an 18V power source, the output of the LVDTs was within a range from 0 to 18 Volt depending on the piston's travel. In order to interpret the measured voltage, the LVDTs needed to be calibrated. For this reason, the LVDT was aligned with a caliper as shown in Figure 3-5. By moving the piston to different positions and measuring a set of displacements and the associated output voltages. Whit this information it was possible to establish a regression line between data points and to determine the slope, m, of the characteristic linear travel-voltage-curve of the LVDTs (Figure 3-6).

Figure 3-5: LVDT calibration setup

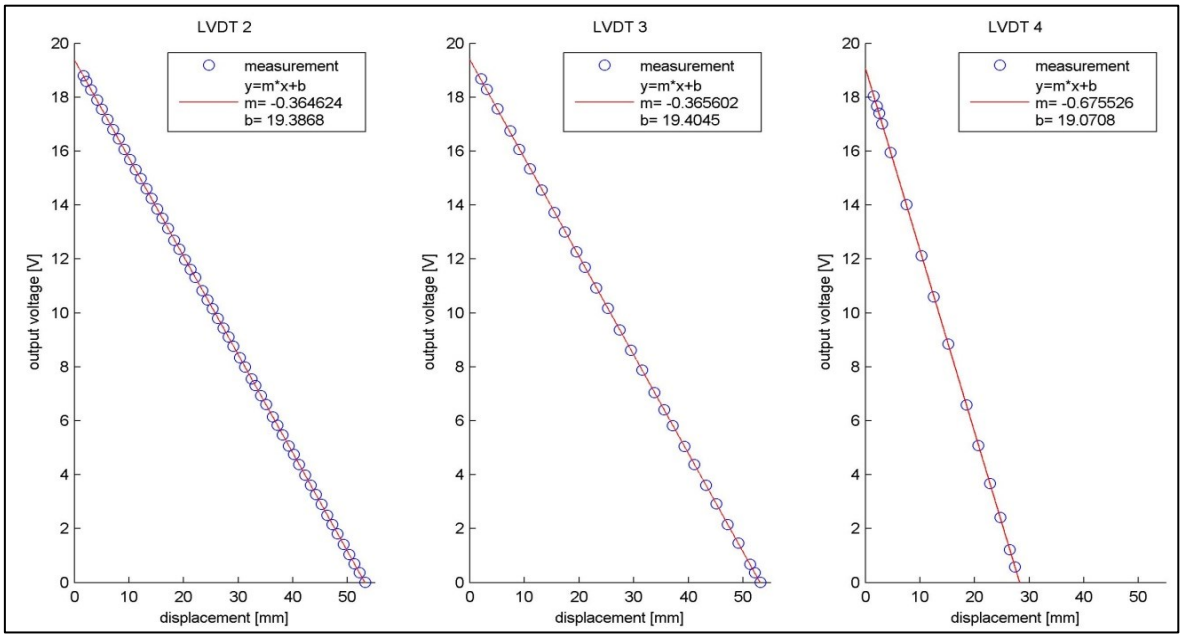

Figure 3-6: LVDT calibration results

Interpreting a difference in two output voltages ΔV as a displacement Δw was now possible:

$$\Delta w = \frac{\Delta V}{m} \qquad 3.1$$

3.2 Model description

The examined connection consists of three self-tapping dowels that link the wooden beam with a 9.5 mm (*3/8 inch*) steel plate, placed at its center. The dowels are placed at a distance u = 107.95 mm (*4.25 inch*) from each other, leaving an edge distance to the upper and lower edge of the beam from about 25.4 mm (*1 inch*). The distance to the end of the beam was 8.255 mm (*3.25 inch*). Figure 3-7 illustrates the placement of the dowels. The minimal distances to the edges of the beam are listed in (Table 3-4).

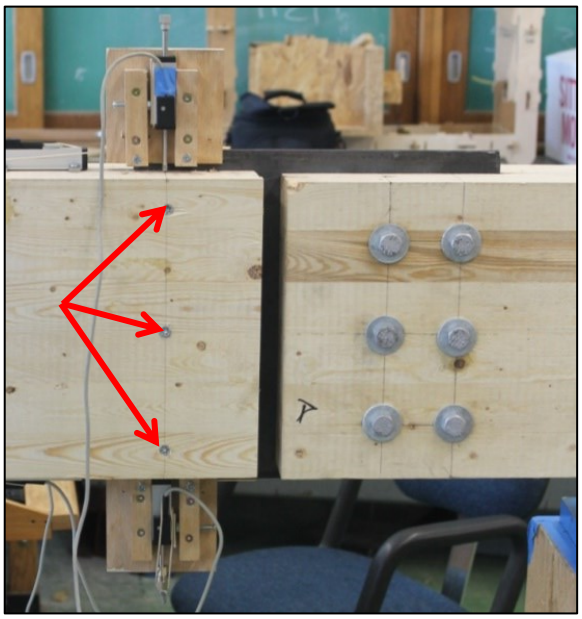

Figure 3-7: Bolts in place

Table 3-4: Minimum Edge- and End-distances according to code

Distance to	**EN 1995-1-1**	**NDS-2015**
Loaded End	/ 80 mm (*3.15 inch*)	7d = 49 mm (*1,93 inch*)
Unloaded End	4d = 28 mm (*1,10 inch*)	4d = 28 mm (*1,10 inch*)
Loaded Edge	4d = 28 mm (*1,10 inch*)	4d = 28 mm (*1,10 inch*)
Unloaded Edge	3d = 21 mm (*0.83 inch*)	1.5d = 10.5 mm (*0.41 inch*)

The whole setup has a span of 2 m (*6.56 ft.*) between the bearings and is loaded in the center at 1 m (*3.28 ft.*). The connection takes place at 0.5 m (*1.64 ft*.), which equals 1/4 of the 2 m span (Figure 3-8). This forces the connection to experience both shear and moment. To minimize the expenses, the steel connecting plate was kept as small as possible; six bolts with a diameter of 12.5 mm (*1/2 inch*) connected it to a small timber end-beam.

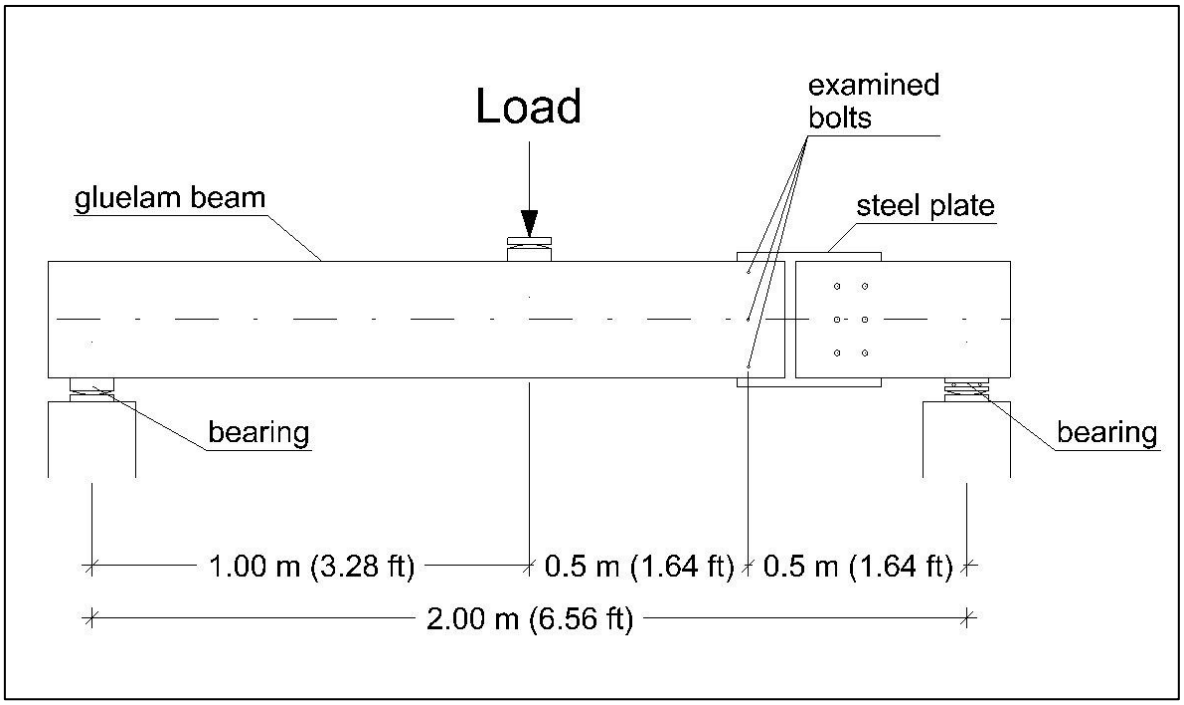

Figure 3-8: System sketch

By design, the weakest part of this setup is the connection with the three self-tapping bolts; failure is expected to occur here. Forces in the connection can be calculated with the following equations due to the applied load F:

$$S = \frac{F}{2} \qquad 3.2$$

$$M = \frac{F}{2} * \frac{L}{4} = \frac{F}{4} \qquad 3.3$$

S… shear force [N]
M… bending moment [Nm]
F… applied load [N]
L… span [m]

Assuming ideal conditions and equal bearing in all holes, the shear force is distributed equally to the three dowels, whereas the moment is split into a force couple acting at the top and bottom bolt. Figure 3-9 shows the resulting force vectors at the bolts.

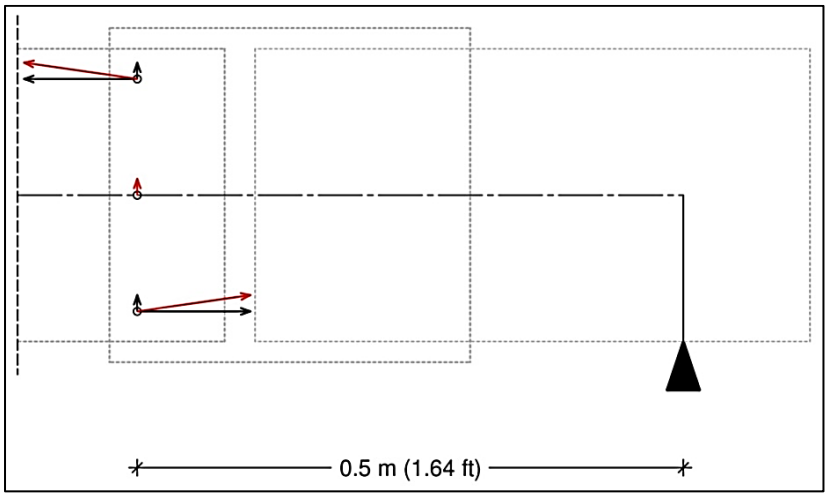

Figure 3-9: Force distribution at the connection (red) vertical and horizontal components (black)

The center bolt is loaded with a force of 0.167 * F and stresses the timber perpendicular to the grain. The top and bottom bolts are loaded with a force equal to 1.186 * F at an angle of 8.02 degrees to the grain.

Due to those forces, the connection will have the following types of deformation:

- Vertical deviation Δd due to shear
- Rotation α due to moment

A spring-based model, like the one in Figure 3-10, can be established. The European code provides formulas to calculate a stiffness value, K_{ser}, for each dowel; using K_{ser} as the base, the displacement of the connection can be estimated.

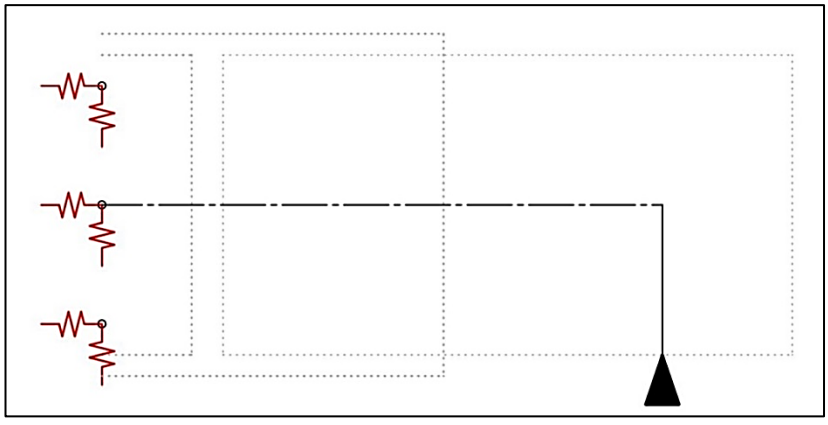

Figure 3-10: Series of springs

For the setup in this thesis, K_{ser} is calculated as:

$$K_{ser} = {\rho_m}^{1.5} * \frac{d}{23} = 430^{1.5} * \frac{7}{23} = 2'713.769\ N/mm \qquad 3.4$$

As this value, per definition is "per shear plane", it must be multiplied by the number of shear planes in the connection. The actual expected deformations, Δd [mm], due to shear and rotation, α [°], can be calculated with the following equations:

$$\Delta d = \frac{S}{K_{ser} * 6} = \frac{F}{K_{ser} * 12} \qquad 3.5$$

$$\alpha = \arctan\left(\frac{\frac{M}{4 * u * K_{ser}}}{u}\right) = arctan\left(\frac{\frac{F}{16 * u * K_{ser}}}{u}\right) \qquad 3.6$$

F… applied load [N]

K_{ser}… spring constant [N/mm]

u… distance from bolt to bolt [mm]

Evaluating these formulas with a load F from 0 to 5'000 N (*1'123.66 lb.*) a load-deflection-curve and a load-rotation-curve can be drawn (Figure 3-11).

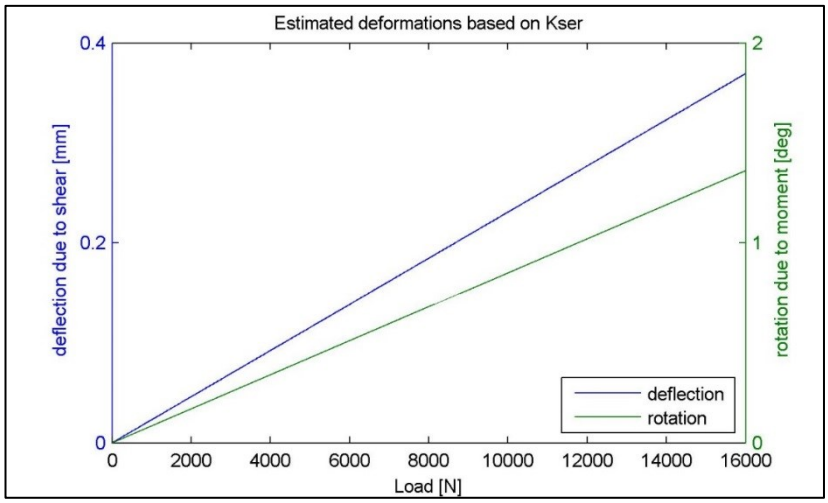

Figure 3-11: Deflection and rotation estimated according European code

As mentioned in Chapter 1, the K_{ser} -value provides only information for linear elastic behavior; this leads to imprecise estimations when plastic deformation takes place. A preferred approximation of the problem is possible by considering the dowels as a bedded beam. Hochreiner [9] describes this method using commercial static software.

4 Single Bolt – embedment testing

4.1 Specimen dimensions

The testing for the single bolt embedment strength was performed as described in EN 383 and ASTM D 5764 (Chapter 2.2). Specimen dimensions were selected to meet the criteria for both codes.

Table 4-1: Specimen dimensions

Load	**Length** [cm (*inch*)]	**With** [cm (*inch*)]	**Thickness** [cm (*inch*)]
Parallel to grain	10 (*3.34*)	7 (*2.76*)	12.5 (*1/2*)
Perpendicular to grain	30 (*11.81*)	7 (*2.76*)	12.5 (*1/2*)

In order to reuse the bolts and perform more than one test with each bolt, it was important not to overload the bolts. For that reason, both codes allow for selecting the thickness of the specimen over a wider range. The thickness was chosen in order that the resulting elastic bending moment would not exceed the maximum elastic bending capacity of the bolt. The characteristic plastic bending moment of the bolts, according to the Rothoblaas datasheet is M_{yk} = 31'930 Nmm (*23.55 lb.ft.*), which leads to an elastic bending moment of approximately 18'808 Nmm (*13.87 lb.ft.*). The transition from plastic to elastic moment for circular cross sections can be calculated as follows:

$$\frac{M_{pl}}{M_{el}} = \frac{\frac{d^3}{6} * f_y}{\frac{\pi * d^3}{32} * f_y} = \frac{16}{3 * \pi} \qquad 4.1$$

$$M_{el} = 31'930\ Nmm * \frac{3 * \pi}{16} = 18'808\ Nmm \qquad 4.2$$

The resulting elastic moment was estimated by assuming the dowel to be a beam loaded with a distributed load, L, spanning the thickness of the specimen plus 0.5 mm (*≈1/64 inch*) clearance. The bearing strength, $f_{h,}$ of the wood was estimated with the European Code formula (Equation 4.3) and based on the maximum expected density, ρ. The characteristic density of Lamboo is ρ_c=670 kg/m^3, but in order to accommodate an estimated 10% variation to this value, ρ=730 kg/m^3 was chosen.

$$f_h = (\rho_c * 1.1) * 0.082 * (1 - 0.01 * d) \qquad 4.3$$

$$f_h = \left(730 \frac{\text{kg}}{\text{m}^3}\right) * 0.082 * (1 - 0.01 * 7\ mm) = 55.67\ MPa \qquad 4.4$$

Multiplying the estimated bearing strength by the dowel diameter, d, results in the distributed load.

$$L = f_h * d = 55.67\ MPa * 7\ mm = 389.69\ N/mm \qquad 4.5$$

The maximum expected moment in the bolt was calculated and compared to the maximum moment specification provided by the manufacturer. In order to not overload the bolt, the maximum thickness of the specimen was limited to 19 mm (*0.75 inch*). However, after performing these calculations, a series of pretests demonstrated a problematic outcome (Figure 4-1).

Figure 4-1: Destroyed bolt after pretests

As a result, the thickness of the specimen was reduced to 12.5 mm (*1/2 inch*).
After establishing the correct dimensions, the selection of wood for the specimen was made by eliminating the pieces with failures; a significant difference was observed between the three materials.

Lamboo had the optimum result; no samples demonstrated failures. This was not surprising considering that bamboo is a uniform base material with only the material between the nodes used to produce the finished product.

White Ash, the only non-engineered material, had significant failures due to notches and holes, but it was still possible to collect enough pieces with sufficient quality for the testing purposes.

Making the specimen from Black Spruce (cut out of a glulam beam) was more challenging, because the material exhibited the most notches and failures. However, this does not mean that the glulam beam was made from a poor material; rather, the material was optimal for a large beam, where small failures are of minimal consequence, but for the relatively small specimens used in this test program they failures were significant. Nevertheless, it was still possible to produce a complete testing set consisting of the required forty specimens with the requisite quality.

For additional calculations, the dimensions of the specimens were recorded. For accuracy reasons, each dimension (length, width and thickness) was measured with a caliper at three different points. The final values represent the average of these three measurements (Table 4-2). Even though the specimens were produced with care, a small variation in the dimensions was observed. Taking into account that the specimens were produced with heavy woodworking tools, such as a circular saw, the variation is tolerated.

Table 4-2: Specimen dimensions - statistics

Dimension	**Target** [mm (*inch*)]	**Actual Average** [mm (*inch*)]	**Minimum** [mm (*inch*)]	**Maximum** [mm (*inch*)]	**Variance** [mm (*inch*)]
Length	100 (*3.34*)	100.31 (*3.95*)	99.93 (*3.93*)	101.04 (*3.98*)	0.07 (*0.0028*)
	300 (*11.81*)	300.14 (*11.82*)	298.89 (*11.77*)	300.87 (*11.85*)	0.23 (*0.0091*)
Width	70 (*2.76*)	69.80 (*2.75*)	68.25 (*2.69*)	71.22 (*2.80*)	0.45 (*0.0177*)
Thickness	12.5 (*0.49*)	12.72 (*0.5*)	11.99 (*0.47*)	13.28 (*0.52*)	0.09 (*0.0035*)

4.2 Numeration

In the testing program a total of 120 individual tests were performed for a total of 120 specimens. Three different materials were tested according to two different testing codes and loaded in two different directions (parallel and perpendicular to the grain). Table 4-3 gives an overview on the distribution and quantities of specimens.

Table 4-3: Overview specimens

Total Specimen	**120**																							
per Material	40								40								40							
per Code	20				20				20				20				20				20			
per Direction	10		10		10		10		10		10		10		10		10		10		10		10	
per Sample	5	5	5	5	5	5	5	5	5	5	5	5	5	5	5	5	5	5	5	5	5	5	5	5

An identification number "x-x-x-x-x" was given to each specimen, which supplied the following information:

- Material "**X**-_-_-_" 1 = White Ash, 2 = Lamboo, 3 = Black Spruce
- Code "_- **X** -_-_" a = ASTM D5764, e = EN 383
- Load direction "_-_-**X** -_" 0 = parallel, 90 = perpendicular
- Specimen No. "_-_-_-**X** " 1 to 10

For example "2e905": Lamboo - tested according to EN 383 - perpendicular to grain – number 5.

Five specimens are grouped in each sample.

Table 4-4: Overview samples

Total samples	**24**											
per material	8				8				8			
per code	4		4		4		4		4		4	
per direction	2	2	2	2	2	2	2	2	2	2	2	2

Sometimes identification numbers may appear in the form "x-x-x-x-x_x"; in these instances the final number in the series (specimen number) was modified into a number containing sample-number and specimen-number (Table 4-5).

Table 4-5: Conversion specimen number with and without sample information

excluding sample information	1	2	3	4	5	6	7	8	9	10
including sample information	1_1	1_2	1_3	1_4	1_5	2_1	2_2	2_3	2_4	2_5

4.3 Testing procedure

4.3.1 Conditioning

Once all specimens were fabricated, they were stored in an environmental chamber, maintaining temperature and humidity at a constant level.

According to EN 383:

- T = 20 ± 2 °C (*68 ± 3.6 °F*)
- H = 65 ± 5 %

Periodically, the specimens weight were recorded until at such time when a constant value was reached where the difference in weight after 6 hours was less than 0.1% of the specimen mass.

$$\Delta m = \frac{m_t - m_{t+1}}{m_t} * 100 \qquad 4.6$$

This conditioning procedure helps all specimens to arrive at the same moisture content allowing for a consistency for comparisons between specimens.

4.3.2 EN 383

As the European code requires the cycling of the load to certain maximum load values (Chapter 2.2.1), it was necessary to estimate a maximum expected load ($F_{max,est}$). To do so, the maximum loads from the pretests were taken and factored down to the new specimen thickness, i.e. multiplying by 12.5 mm / 19 mm = 0.66.

Based on $F_{max,est}$ the required testing speed was then calculated. The code requires that the time for the final loading cycle (from 0.1 * $F_{max,est}$ to $F_{max,est}$) takes 300 (±120) seconds. However, as the MTS testing machine is displacement controlled, the testing speed had to be calculated as displacement/time (mm/min). In the pretests, a displacement of approximately 4 mm (*0.157 inch*) was noticed from 0.1 * $F_{max,est}$ to $F_{max,est}$, so the testing speed was set to:

$$v = \frac{4\ mm}{300\ s} = \frac{4\ mm}{5\ min} = 0.8\ mm/min \qquad 4.7$$

A constant speed was maintained for all loading and unloading processes. It was only adjusted, if the previous test demonstrated that the maximum load was reached too quickly.

To measure the deformation, the LVDT was attached to the unloaded side of the specimen and the deformation relative to an aluminum angle, attached to the steel bearing blocks, was point of measure (Figure 4-2 and Figure 4-3).

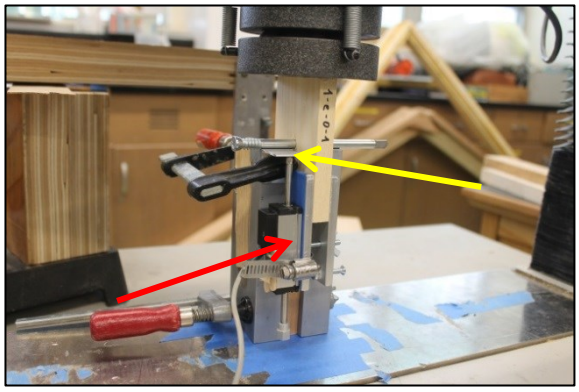

Figure 4-2: LVDT assembly (a)
LVDT (red arrow)
Aluminum Angle (yellow arrow)

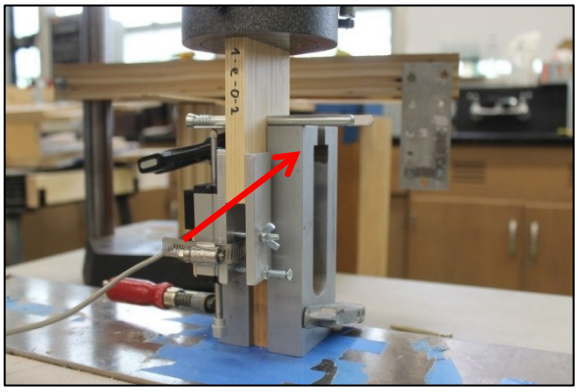

Figure 4-3: LVDT assembly (b)
bearing block (red arrow)

Only one LVDT, small enough to fit in the testing setup, was available during the tests for the White Ash and Lamboo specimen; therefore, the requirement of two LVDTs was not satisfied. When the tests on the Black Spruce specimens were performed, two LVDTs were available and tested; LVDT data x_{LVDT} for Black Spruce represents the average of the two LVDT readings.

$$x_{LVDT} = \frac{LVDT_1 + LVDT_2}{2} \qquad 4.8$$

4.3.3 ASTM D 5764

For the ASTM D 5764 tests, the requirement was to change the loading procedure to one of constant loading without cycling. Even though the American code requires the measurement of the displacement at different points, the LVDT configuration was kept the same as in EN 383 tests. The reason for keeping the setup the same was because the crosshead displacement was already recorded by an internal sensor of the machine. By not changing the LVDT setup, it was possible to also compare the LVDT data.

4.3.4 Data corrections

To avoid failure due to the deformations in the machine frame and the steel bearing blocks a test was performed (Figure4-4) in order to calculate the "setup stiffness" k_{setup}. The value for k_{setup} was 133.73 kN/mm (*763'674.62 lb./inch*).

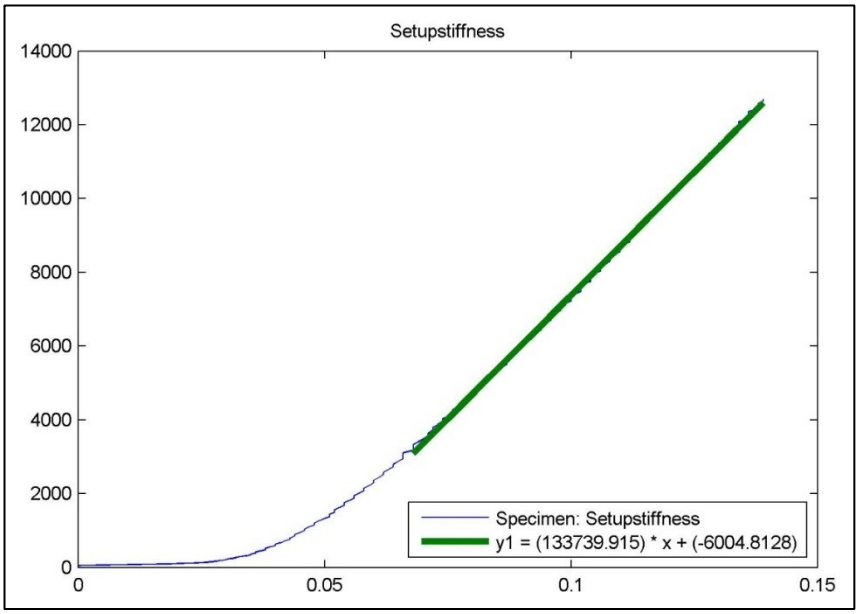

Figure4-4: Setup stiffness

All additional Crosshead values, $x_{Cross,}$ have been corrected by subtracting a displacement, $\Delta x_{setup,}$ proportional to the Load, L, and the setup stiffness, k_{setup}.

$$x_{Cross} = x_{Cross} - \Delta x_{setup} = x_{Cross} - \frac{L}{k_{setup}} \qquad 4.9$$

After the tests were performed, the specimens were dried in a ventilated oven at a temperature of 103 °C (*217.4 °F*) until a constant weight was reached. This weight represents the dry weight (w_{dry}) of the wood; the difference between the weight, $w_{test,}$ at test time and w_{dry} compares to the weight of the moisture and the percent of relative moisture content can be calculated.

$$m = \frac{w_{test} - w_{dry}}{w_{test}} * 100 \qquad 4.10$$

4.4 Results

Uncertainties exist with each observation; repeatedly measuring the same value will result in slightly different results. This is especially true for timber and timber based products, as certain variations are intrinsic to their properties. Table 4-6 provides a summary of the observed data:

Table 4-6: Results – dry density and moisture content at test

Material	Number of tests	Average dry density [kg/m³]	Standard deviation density [kg/m³]	Density 5% quantile[4] [kg/m³]	Average moisture content [%]	Standard deviation m.c. [%]
White Ash	40	609.62	68.90 (11.35%)	494.48	10.24	0.56
Lamboo	40	624.16	28.59 (4.58%)	577.43	6.42	0.55
Black Spruce	40	520.19	25.10 (4.83%)	481.67	13.10	1.02

The data demonstrates a clear difference referencing density; Black Spruce, which is the only softwood in this comparison has the lowest density; it is about 15 % lower than the density of White Ash, which is a hardwood. Lamboo, being neither a hard nor a soft wood but a grass also has a relatively high density, similar to White Ash - difference approximately 2.3 %.

The deviation in the densities underscores the fact that Lamboo and Black Spruce are engineered products. Due to the selective process, the standard density deviation is less than 5%, whereas the standard deviation of White Ash is over 10 %. Characteristic values were calculated as 5% quantiles, assuming a standard normal distribution[5]. However, the manufacturer's technical data demonstrates a difference from those results; which may be attributed to the relatively small sampling set tested in this thesis (Table 4-6 to Table 4-8).

[4] 5% quantile of dry density

[5] In the European code standard normal distribution is used for the determination of characteristic density, whereas standard logarithmic normal distribution is used for characteristic strength values

Table 4-7: Comparison average measured density and density from literature m.c. = 12 %

Material	Measured average density [kg/m³]	Literature [kg/m³]
White Ash	620.35	670
Lamboo	658.99	673 [6]
Black Spruce	520,47	410

Comparing the measured densities with the related literature (Table 4-7 [13] [14]), a relatively big difference can be observed. This difference could again be caused by the relatively small amount of test-specimen.

Table 4-8: Indication of density according to Nordic's datasheet[7]

Applied code	Characteristic density ρ_k [kg/m³]	Mean relative density G [ ]
EN 1995-1-1	430	/
NDS 2015	/	0.46

The moisture content at test time was calculated over the weight at test time and the dry density of the material (Equation 4.10). Although the relative humidity could not be controlled during the seasoning of the Black Spruce specimens, the moisture content was within an acceptable range - approximately 12%. It is interesting to see that Black Spruce and White Ash, both are timbers, resolve to similar moisture contents, whereas Lamboo's moisture content is much lover. A reason for this might be the different cellular structure of bamboo and a different affinity to water of the material. The inability to control moisture content during the conditioning process resulted in the elevated standard deviation of moisture content in the Black Spruce specimens, which is double compared to the other materials.

[6] Density according manufacturer's datasheet
[7] Black Spruce

Table 4-9: Results - bearing strength

Material	Characteristic density[8] [kg/m³]	Code	Load direction	Average bearing strength [MPa]	Standard deviation [MPa]	Min bearing strength [MPa]	Max bearing strength [MPa]	Diff. in bearing strength [%]
White Ash	503.18	EN 383	par.	53.37	8.45 (15.83%)	41.18	68.44	100
			perp.	70.25	16.13 (22.96%)	55.09	103.69	100
		ASTM D5764	par.	38.78	7.50 (19.35%)	28.37	50.37	72.66
			perp.	29.68	5.57 (18.78%)	22.55	37.87	42.25
Lamboo	609.65	EN 383	par.	60.22	9.41 (15.63%)	47.77	76.86	100
			perp.	71.70	7.64 (10.65%)	61.04	81.93	100
		ASTM D5764	par.	52.58	5.50 (10.46%)	42.47	58.42	87.31
			perp.	40.30	10.44 (25.91%)	24.66	52.53	56.21
Black Spruce	476.37	EN 383	par.	21.03	2.73 (12.67%)	16.32	23.86	100
			perp.	32.57	3.43 (10.52%)	28.35	37.29	100
		ASTM D5764	par.	22.47	2.87 (12.77%)	17.42	27.96	106.85
			perp.	15.99	1.94 (12.14%)	13.80	20.11	49.09

[8] 5 % quantile of average density at moisture-content of 12 %

The standard deviation in bearing strength for all the tests was within the range of 10 to 25 percent. No distinct difference could be observed between the materials. Additionally, between the two codes, no significant difference in the standard deviations was observed. Taking a closer look at the difference in average bearing strength, the effects of the different approaches gathering the maximum load in each code can be observed. Parallel values differ in a range from 6.85 % to 27.34 % whereas values with a perpendicular load direction show differences from 43.79 % up to 57.75 %.

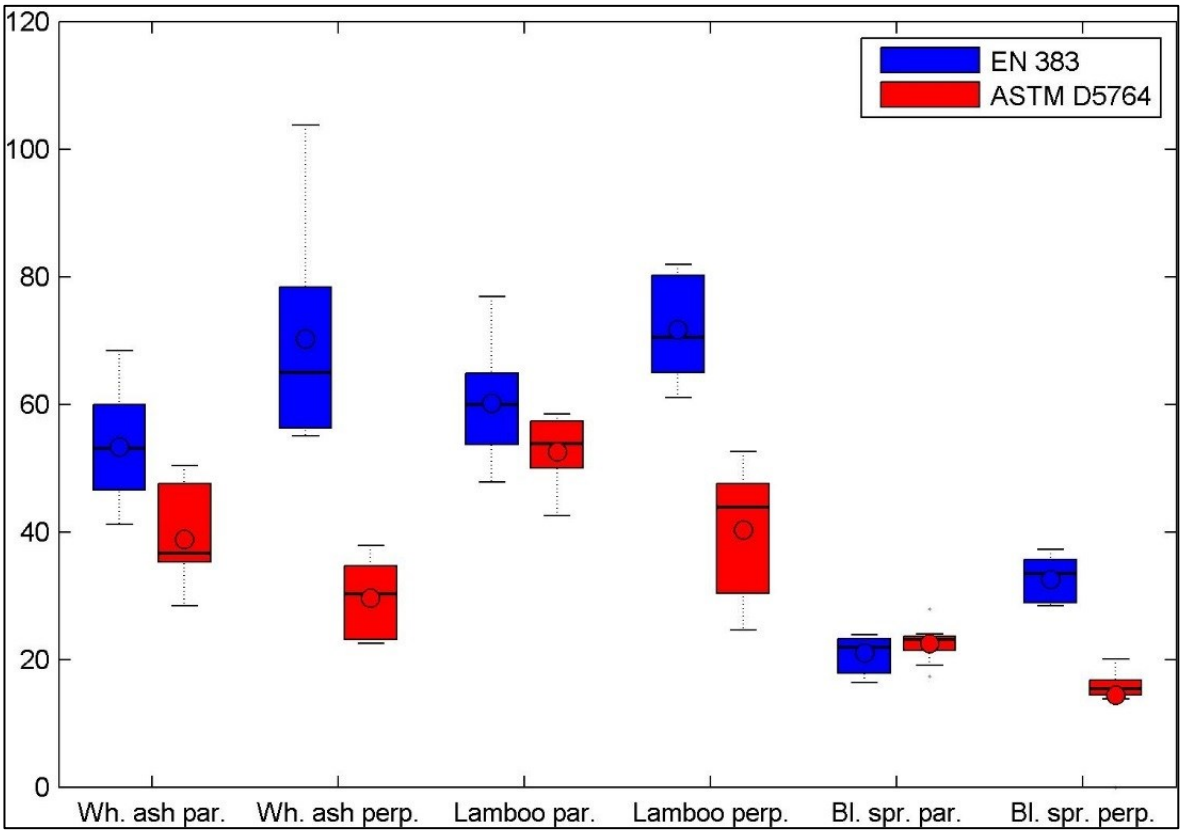

Figure 4-5: Results - comparison statistics of bearing strength [N/mm²]

Bearing strength results (Figure 4-5 & 4-6) demonstrated a trend toward greater densities.

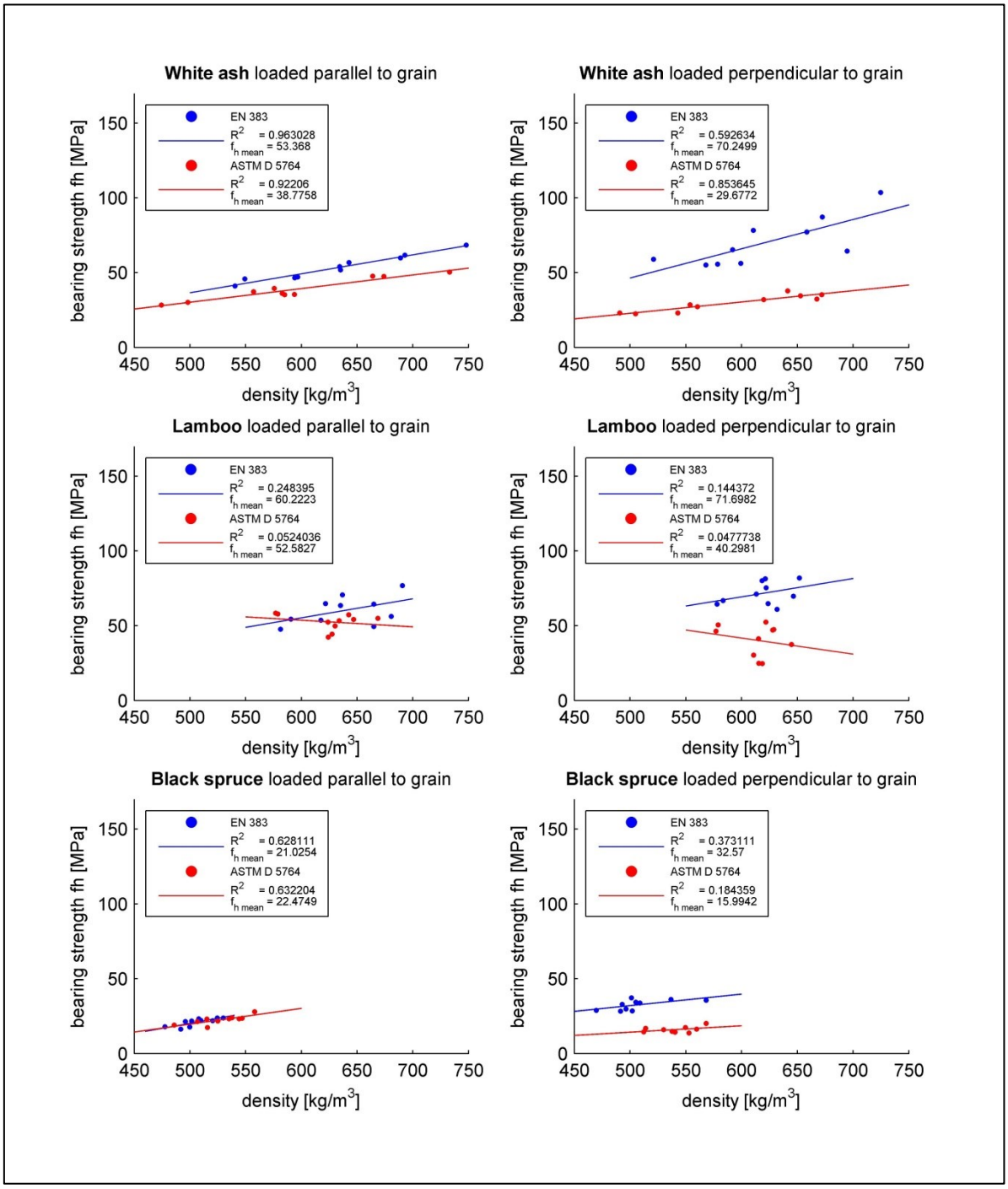

Figure 4-6: Comparison EN 383 and ASTM D 5764 – bearing strength over density

With additional simulations and calculations, load-displacement-density (LDD) surfaces were created, collecting load displacement curves and organizing them based on the dry density.

These LDD surfaces then were "smoothed" by executing a linear interpolation to the densities. Based on these surfaces it was possible to obtain load-displacement curves for variable input densities by slicing the surface at the desired density. Figure 4-7 to Figure

4-10 demonstrate the elaborated LDD surfaces with the calculated load-displacement curves according to the mean densities displayed (Table 4-6).

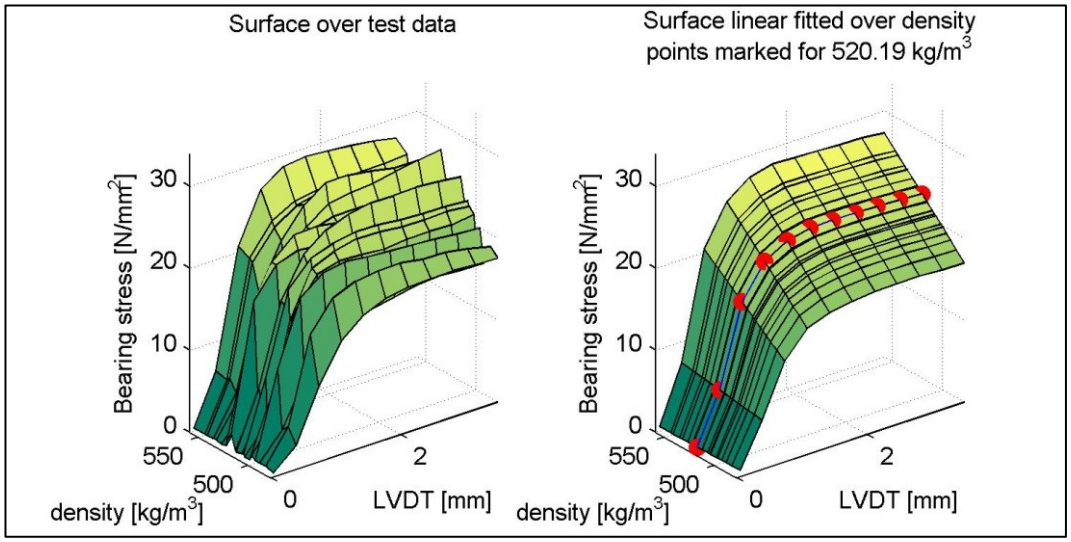

Figure 4-7: LDD surface parallel to grain - EN 383

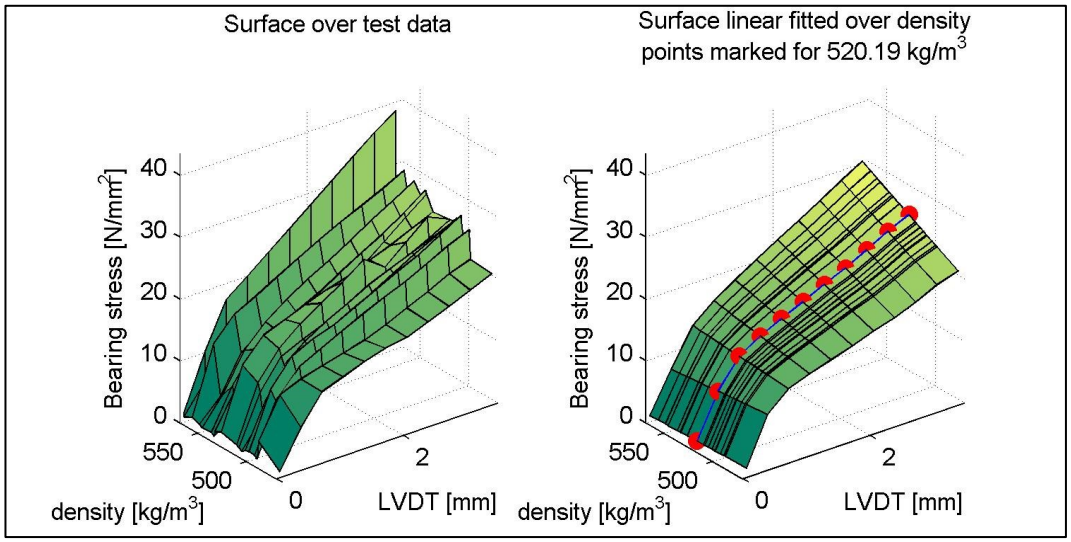

Figure 4-8: LDD surface perpendicular to grain - EN 383

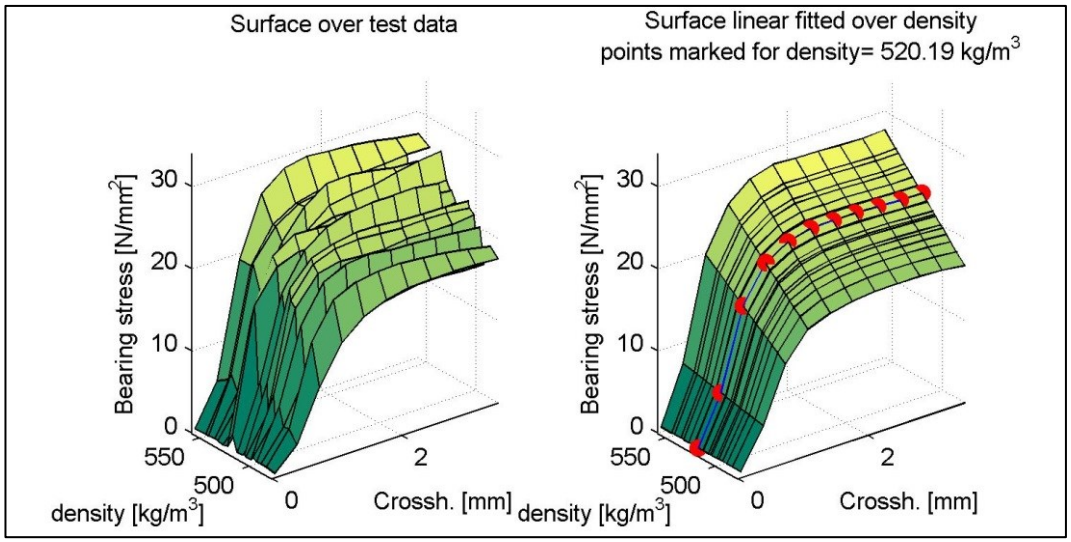

Figure 4-9: LDD surface parallel to grain - ASTM D 5764

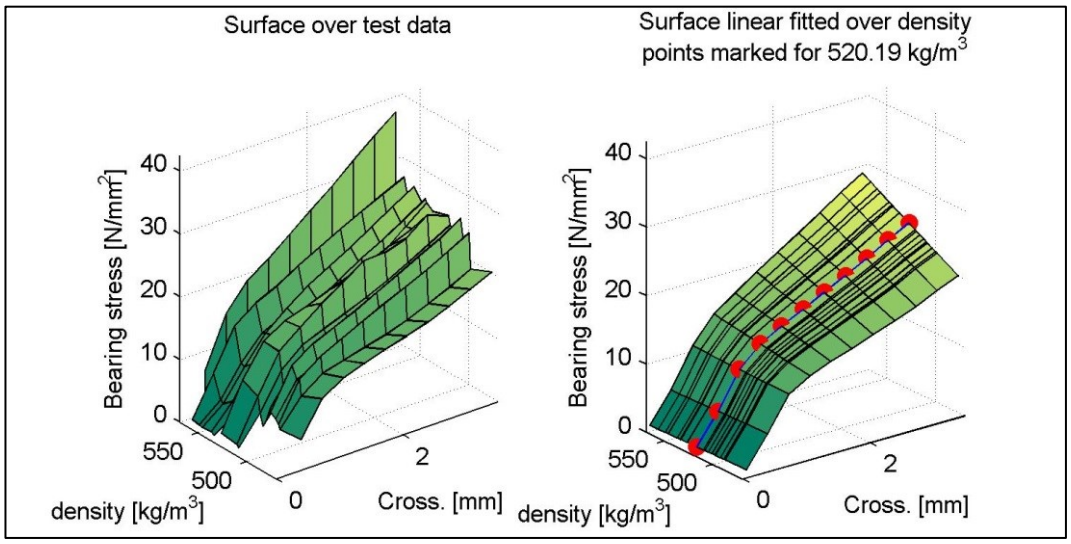

Figure 4-10: LDD surface perpendicular to grain - ASTM D 5764

Even though both codes attempt to establish specimen dimensions minimizing splitting, a significant sample of the White Ash (25%) and Lamboo (75%) specimen showed a brittle failure mode when loaded parallel to grain. Figure 4-11 illustrates a damaged specimen and Figure 4-12 demonstrates the corresponding load-displacement-graph.

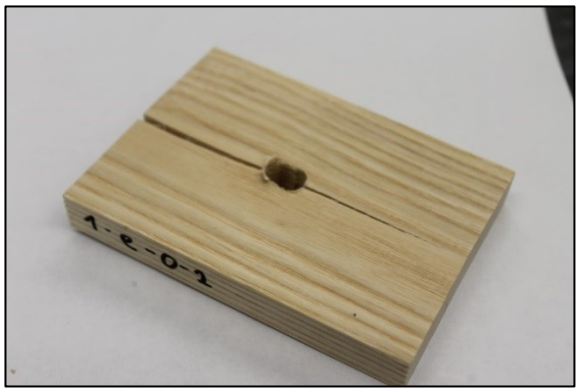

Figure 4-11:
Specimen with splitting failure

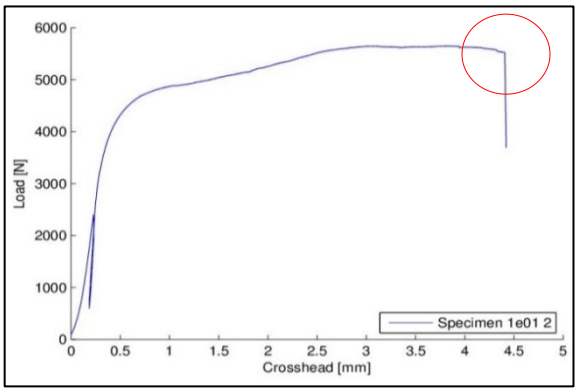

Figure 4-12:
Sign of splitting failure in parallel loaded tests

The rest of the specimens did not fail as a result of splitting; rather, the failure mode was characterized by "tearing" the dowel through the wood. Especially in tests where the load was applied perpendicular to grain where an initial compression of the fibers was followed by a tensile rupture of the fibers (Figure 4-13). This tensile rupture can be observed in the load-displacement curves (Figure 4-14).

Figure 4-13:
Specimen with tensile rupture of fibers

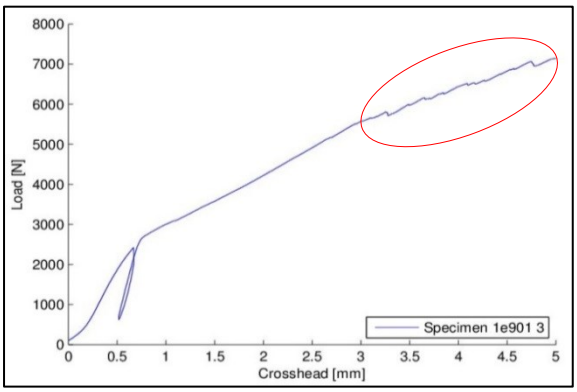

Figure 4-14:
Signs of tensile rupture in perpendicular loaded tests

Both codes provide similar values referencing the bearing strength parallel to grain, however for the tests where the load is applied perpendicular to the grain, the results show a significant difference. Figure 4-6 illustrates the difference (results parallel to grain are shown at the left results perpendicular to the right).

The reason for this difference is that the second straight line in the load-displacement curve (Figure 4-12) is nearly even in parallel loaded tests, whereas it is ascending in the perpendicular loaded tests (Figure 1-3). This leads to far greater ultimate load values than in yield load (Chapter 2.2.2). Taking into account the size of the difference, it is very important to address possible consequences by including bearing strengths that are calculated according to the European Code, EN 383, in the American static calculations. Even though engineers should not make such a mistake, an assimilation of the codes could prevent an inadvertent error and prevent a possibly dangerous eventuality.

5 Connection with fastener-group

5.1 Specimen preparation

In order to examine the stiffness of a fastener-group, five test-specimens with the connection described (Chapter 3.2) were constructed. The large sample sets prohibited the use of the of the climate chamber; however, as wood was stored in the laboratory for approximately one month prior to the tests, a consistent moisture content across all sample sets was arrived.

To construct the connection, a 9.5 mm (*3/8 inch*) slot was cut into the glulam beams with a band saw; an ASTM A36 grade steel plate was inserted into the slot and three bolts were placed. Inserting the self-tapping bolts was a challenge. First, determining that the bolts entered precisely perpendicular to the surface was not possible with a hand-operated drill. A jig was made and a drill press used to achieve satisfactory alignment. Initial skepticism concerning the drilling ability of what appeared to be a fragile drill tip proved groundless. Out of 15 bolts only two did not drill through the 9.5 mm steel, which approached the manufacturer's suggested maximum thickness of 10 mm (*0.39 inch).* It was also difficult to maintain the required pressure on the vibrating machine until the bolt completely penetrated the steel.

Two different failures occurred (Fig. 5-1) while inserting the bolts. One drill tip appeared to be not hard enough as the cutting edge was dulled by the steel plate and required replacement. The second failure occurred at the connection of the drill tip to the steel rod, which resulted in the drill tip breaking off. This second failure was the worst case as when placing this kind of fastener it is impossible to extract the broken drill tip out of the hole allowing for the placement of a new bolt resulting in the complete loss of one test beam.

Figure 5-1: Broken drill-tip

5.2 Testing procedure

The testing procedure for a group of fasteners differs from the single bolt tests described (Chapter 4). Procedure was the same for both, the American and the European code. The testing speed was set to a constant 2 mm/min (*0.0787 inch/min*) as bigger deformations were expected at the loading point. To measure the rotation and displacement in the connection a total of four LVDTs were used. Two of which measured the rotation (Figure 5-2 horizontal LVDTs marked in red) and two measured the vertical displacement (Figure 5-2 vertical LVDTs marked in yellow).

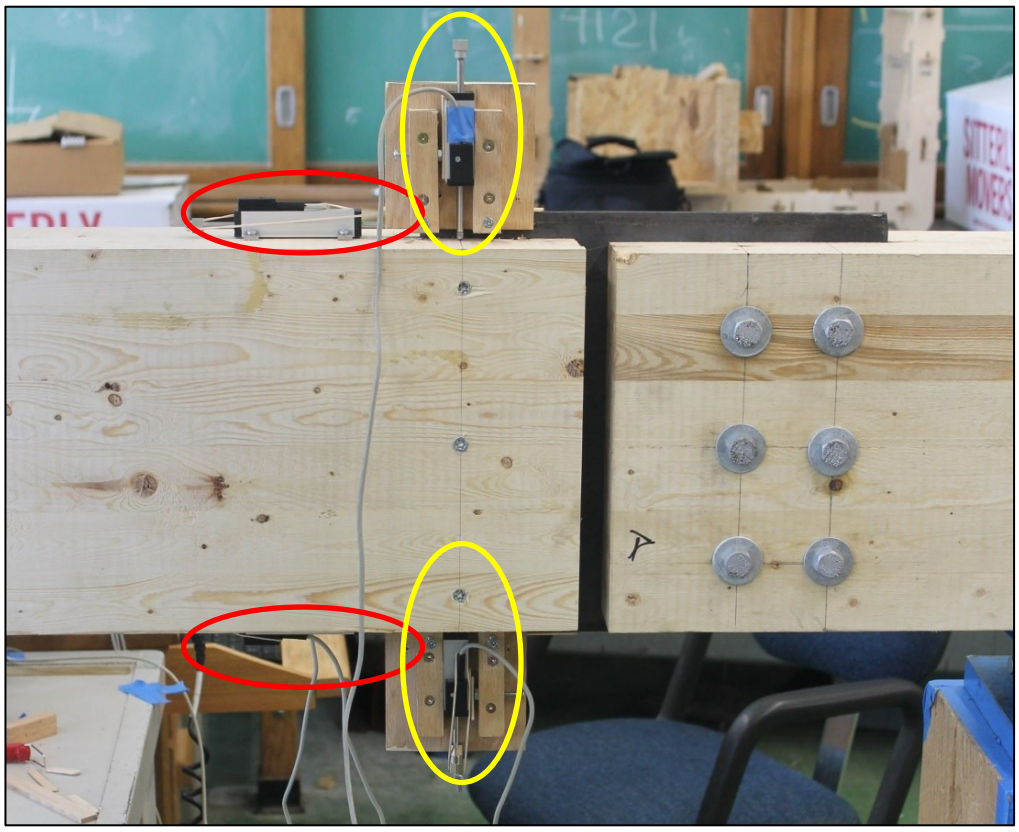

Figure 5-2: Connection with added LVDTs

As the bolts are slender [Length = 133 mm (*5.236 inch*); Diameter = 7 mm (*0.276 inch*)] a distinct ductile behavior was expected, i.e. failure in rotation due to the lower rotational strength of the setup.

After each test, the moisture content was measured with the Delmhorst moisture-meter at several points along the two sides of the connection.

5.3 Results

As a result of a software problem when testing the first of the four specimens, only the results of three tests are represented in this Chapter.

The moisture content observed in the specimen is shown in Table 5-1.

Table 5-1: Moisture content for group tests

Specimen	Readings	Average moisture content [%]	Standard deviation [%]	Coefficient of Variation [%]
G1	/	/	/	/
G2	/	/	/	/
G3	30	9.8	1.2	0.12
G4	35	10	0.47	0.22
G5	35	9.9	0.8	0.08

The moisture content in all specimens was very close, considering the minimal values of the standard deviation and coefficient of variation it is assumed, that all wood arrived at a stable moisture content during the time it was stored in the laboratory.

The data recorded by the LVDTs needed to be interpreted to determine the actual rotation and displacement. To calculate the rotation, the distance Δl between the two LVDTs was measured. The rotation α could then be calculated with the following formula:

$$\alpha = \arctan\frac{LVDT_{upper} - LVDT_{lower}}{\Delta l} \qquad 5.1$$

Figure 5-3 shows the resulting rotation in dependence of the applied load.

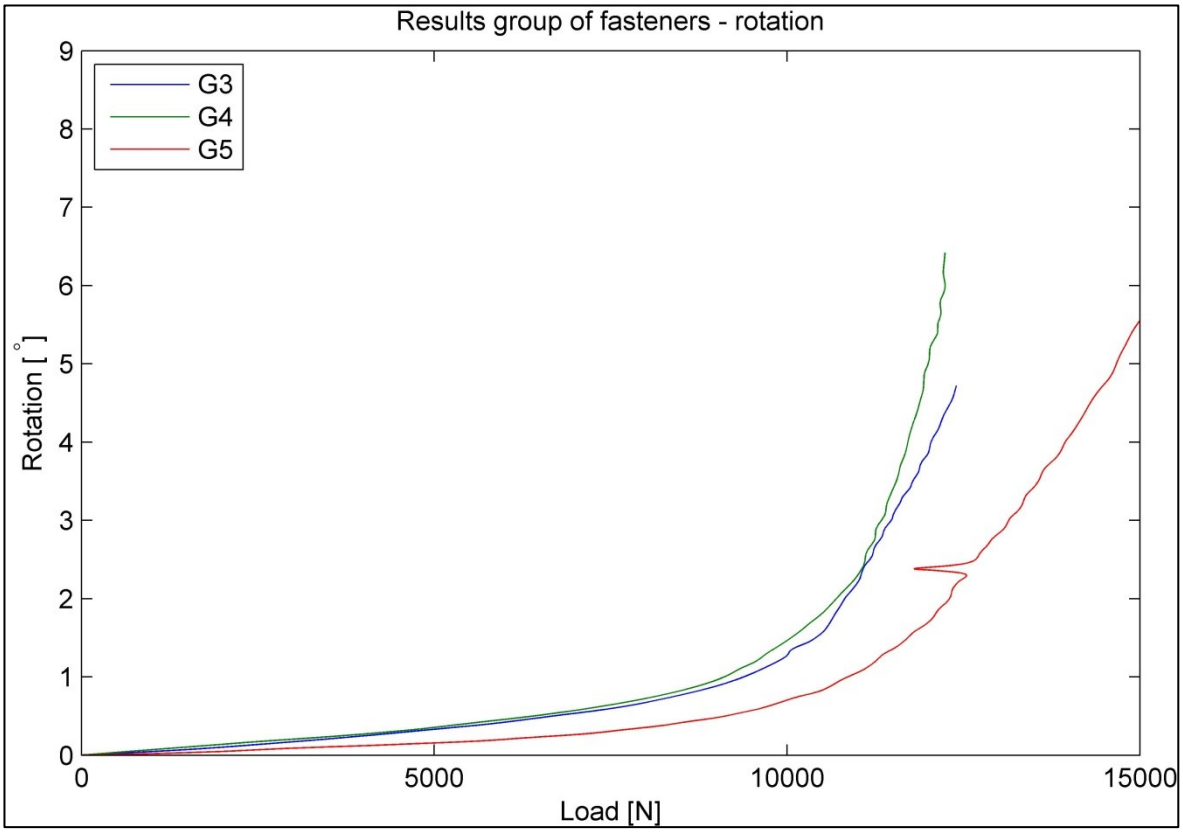

Figure 5-3: Results group of fastener – rotation

Interpreting the results from the two LVDTs that recorded the vertical displacement was more difficult. As a result of the rotation, the angle between LVDTs and the measured surface changed as the measured point traveled from the initial location (Figure 5-4).

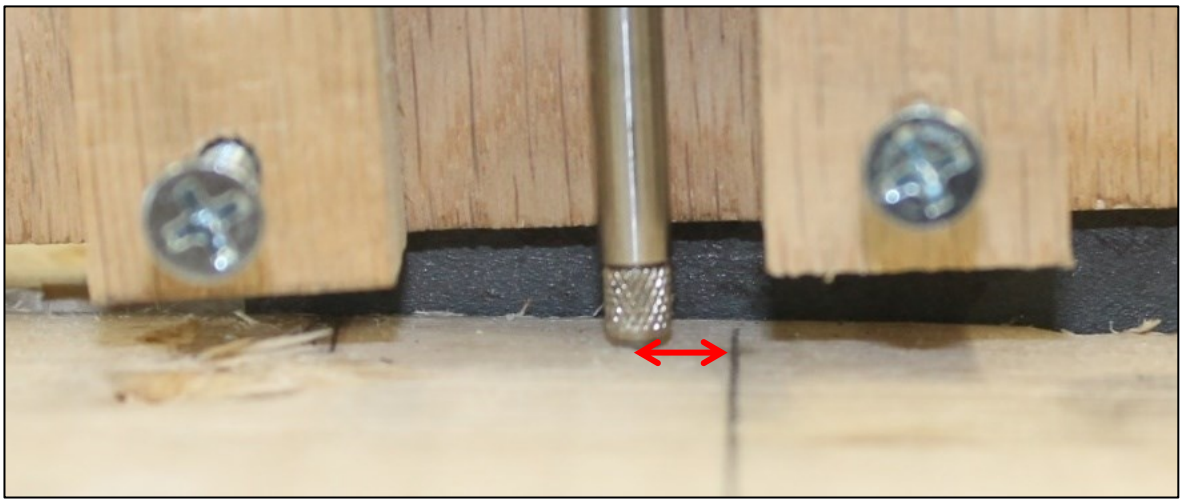

Figure 5-4: LVDT travel

The values measured by the LVDTs not only represent the vertical displacement from steel to wood, but also contain a certain amount of error-displacement due to the rotation.

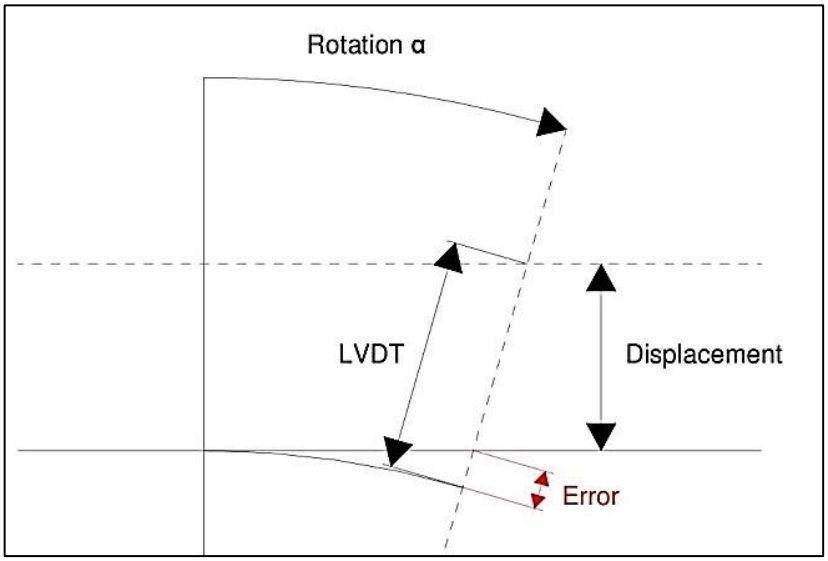

Figure 5-5: LVDT Error due to rotation; upper LVDT

This rotation-based error is shown in Figure 5-5; it was eliminated by applying the following formulas:

Upper LVDT:

$$y = \left[h_{Beam} * \left(\frac{1}{2 * cos(\propto)} - \frac{1}{2}\right) - s_{LVDT}\right] * cos(\propto) \qquad 5.2$$

Lower LVDT:

$$y = \left[s_{LVDT} + h * \left(\frac{1}{2} - \frac{1}{2 * cos(\propto)}\right)\right] * cos(\propto) \qquad 5.3$$

With:

y… Vertical displacement [mm]

h_{Beam}… Height of Beam [mm]

s_{LVDT}… Value measured by LVDT [mm]

α… Rotation angle [°]

An assumption was made that the center of the rotation corresponds with the centerline of the beam at half its height. The contribution to total failure attributed to this assumption is minimal; furthermore, the calculation of the rotation point would require calculating the intersection point of two straight lines that intersect at a very acute angle (Figure 5-3), which would lead to a glancing intersection.

The final displacement was calculated by taking the average of the upper and the lower vertical displacement.

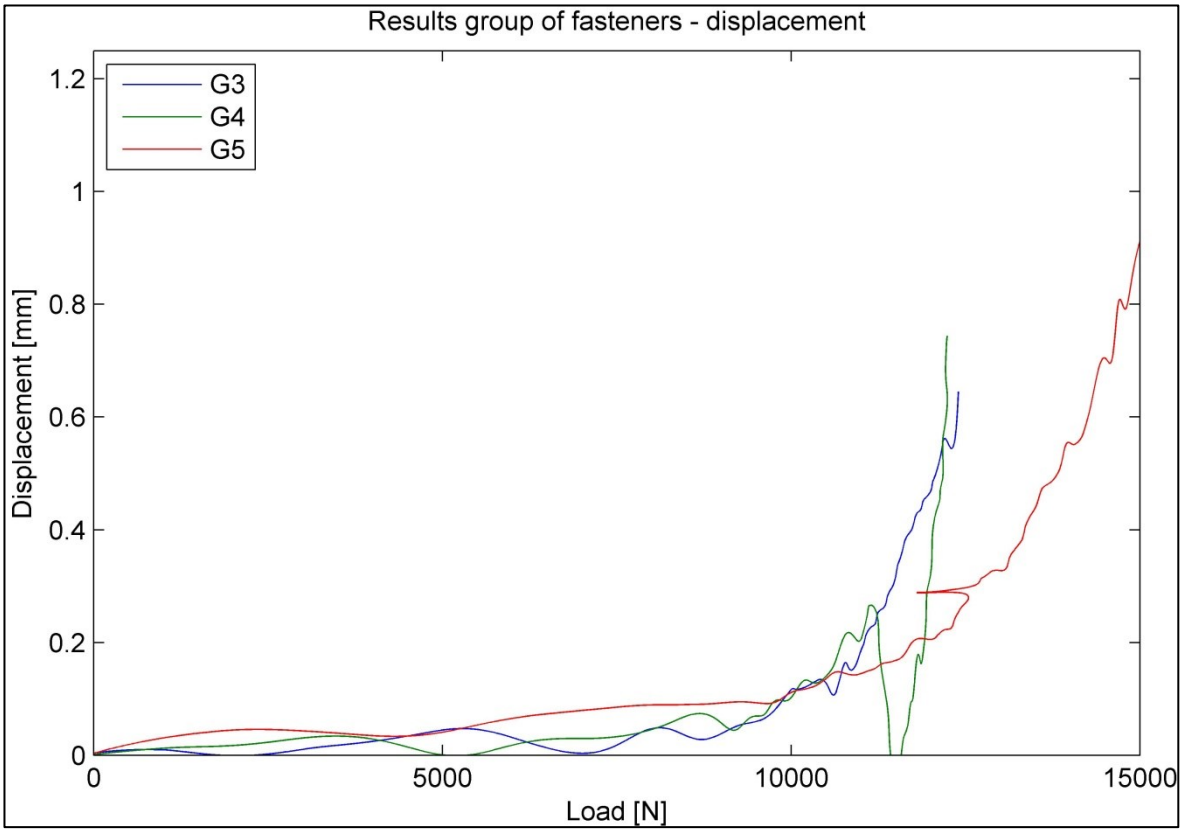

Figure 5-6: Results group of fasteners – displacement

The abrupt drop in the graph of the test results for G3 (green line in Figure 5-6) may have been caused by a slight movement of the LVDT fixture. At all other comparisons the line should not be considered at a load-level above 11'000 N (*2'472.90 lb.ft.*).

5.4 Modeling

5.4.1 RSTAB

The static program RSTAB 8.06 from DLUBAL was used to model the connection. It is a highly regarded and widely used program in engineering offices.

The model consisted out of three parts:

- Cantilever beam
- The bolts
- The bearings

The cantilever beam was used to achieve the desired moment and shear components in the connection by simply adding a single force equal to the bearing load on the tested beam
(Figure 5-7). It was modeled with a length of 500 mm (*19.685 inch*). On the end, where the cantilever beam is attached to the bolts, a distribution construction was modeled so that the forces would act on the bolts at the edges of the steel plate (Figure 5-8). All the beams used for cantilever and distributional construction, are set as weightless rigid members in order to prevent deformation from taking place at this location. Since the size of the steel plate overwhelms the bolt dimensions, and because all of the connection's deformation occurs in the wood-bolt system, this assumption can be made with confidence.

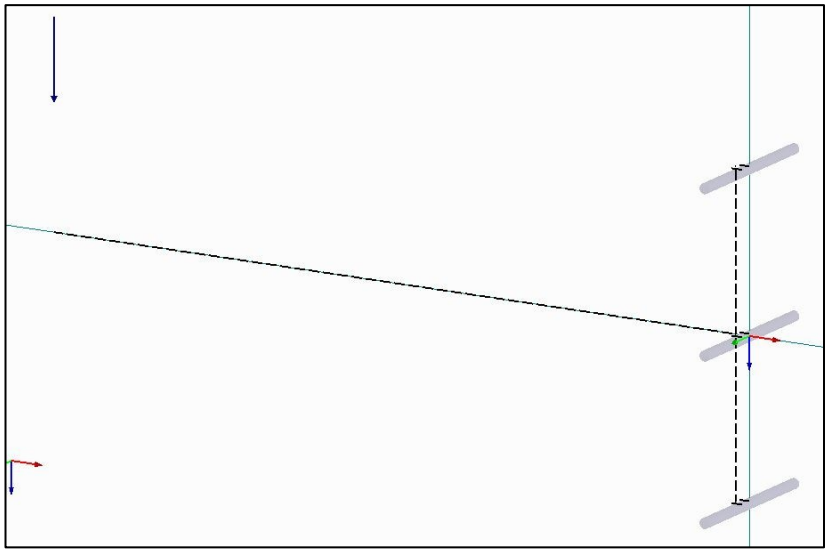

Figure 5-7: RSTAB - Cantilever beam

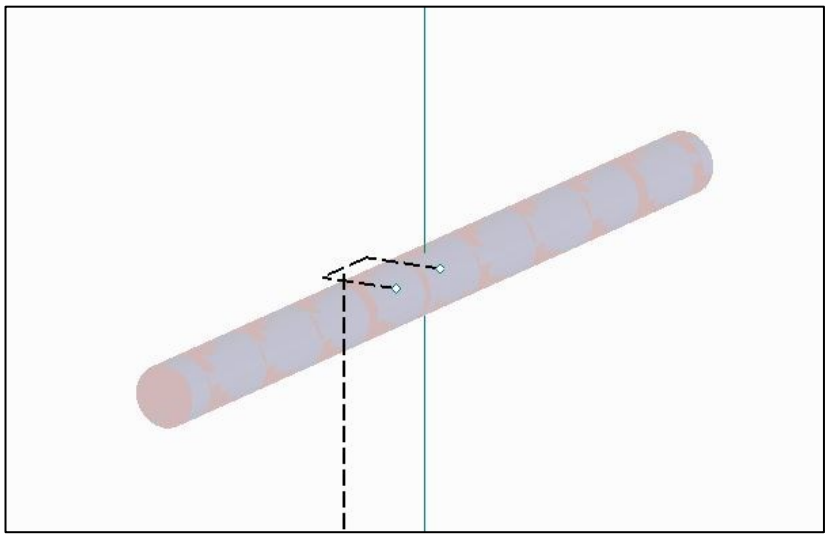

Figure 5-8: RSTAB – Distribution construction (to upper bolt)

The bolts were modeled as steel beams with round cross sections, diameter 7 mm (*0.275 inch*). To simulate behavior as close as possible to the real bolts, values for the development of plastic hinges have been inserted. The manufacturer gives a characteristic yield moment of 31'930 Nmm (*23.550 lb.ft.*) according to EN 409 which was used for the plastic moment in both y and z-directions (Figure 5-9).

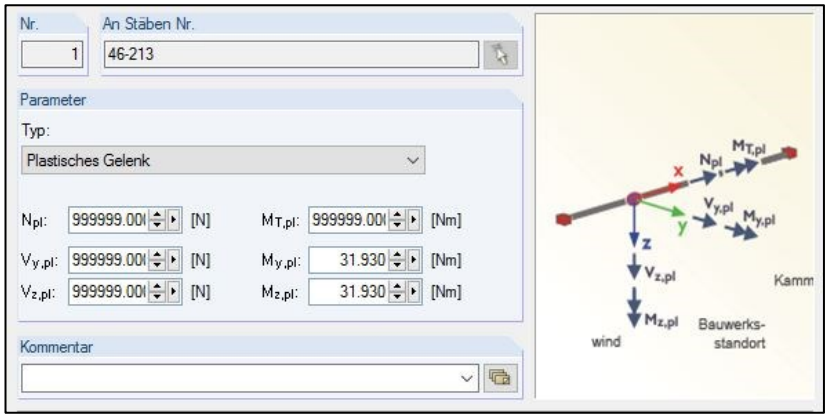

Figure 5-9: RSTAB - Settings for plastic hinges[9]

To represent the embedment in the wood, a set of bearings was modeled (Figure 5-10). The distance between each bearing is set to 2 mm (*0.079 inch*). This dimension is relatively small when compared to the diameter of the bolt in order to get smooth results.

[9] The inputted 999999 values are RSTAB's methodology for removing these inputs from the calculation

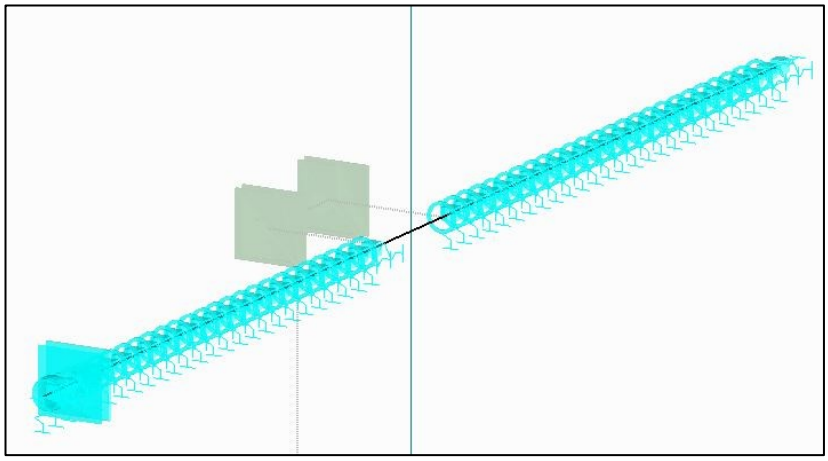

Figure 5-10: RSTAB - Bearings at bolt

Each bearing is designed to simulate the embedment behavior collected in Chapter 4.4. All rotations as well as displacements in y-direction are set to be free[10]. Spring like behavior was inputted for the displacement in x- and z-direction. As the bolts fit so tightly in its bored hole, some amount of axial force is expected due to friction between wood and bolt. The friction coefficient was set to 0.25; the friction force is then calculated in the program by multiplying the y- and z component of the bearing force with this coefficient. In the real life tests, the bolt-heads were slightly forced into the wood, which results in an axial force. Contributing to this effect, the bearing at one end of the bolt was fixed in the y-direction and on the opposite end, a spring was set to 5'000 N/mm (*28'550.74 lb./inch*).

In order to contain the plastic behavior of the embedment (Chapter 1), load displacement curves were used instead of linear spring constants in both x- and z-directions. These load displacement curves are again extracted from the LDD surfaces (Chapter 4.4). As these values are force per area, they needed to be multiplied by the dowel diameter and the distance between each bearing.

[10] Only for stabilizing the numeric behavior of the calculations, a small amount of stiffness (1 Nmm/°) was applied in z-directions rotation.

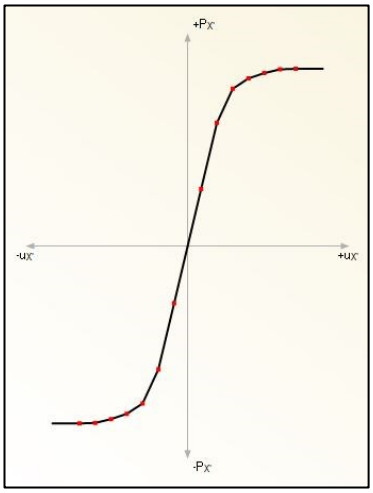

Figure 5-11:
RSTAB - Spring setting for bearing parallel to grain

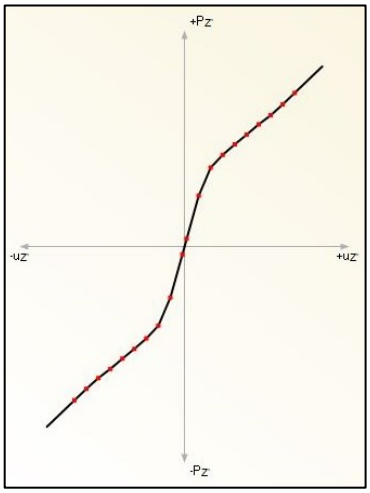

Figure 5-12:
RSTAB - Spring setting for bearing perpendicular to grain

It is possible to set different behaviors, e.g. rupture, for the spring after the last step. The settings for the parallel to grain bearing can be seen (Figure 5-11). As the tests did not indicate any failure due to splitting, the behavior this option was set to "yielding", which creates a horizontal plateau after the last inserted point.

For the perpendicular to grain embedment the situation is different. In this instance, the embedment-tests indicated a hardening in the plastic range, therefore the graph was set to continue with the slope at the last point (Figure 5-12).

All curves were evaluated with the mean density based on the LDD surfaces gathered in the EN 383 and ASTM D 5764 tests.

5.4.2 Calibration

The initial simulations runs were with the original bearing-strength values from the LDD surfaces and the mean densities collected (Chapter 4.4). As Figure 5-13 shows, the simulation did not precisely reflect the test results and required calibration.

After reviewing the model's geometry and the program's settings, no errors were detected leading to an examination of the material settings. A second review of the graph revealed too low stiffness in rotation and displacement could be observed in the simulations. The reason for this low stiffness could be either in the bolt's material or in the settings for the embedment. Since the materiality of steel is well understood and shows small deviations in characteristic properties, the assumption was made that the specifications supplied by the manufacturer should be trusted.

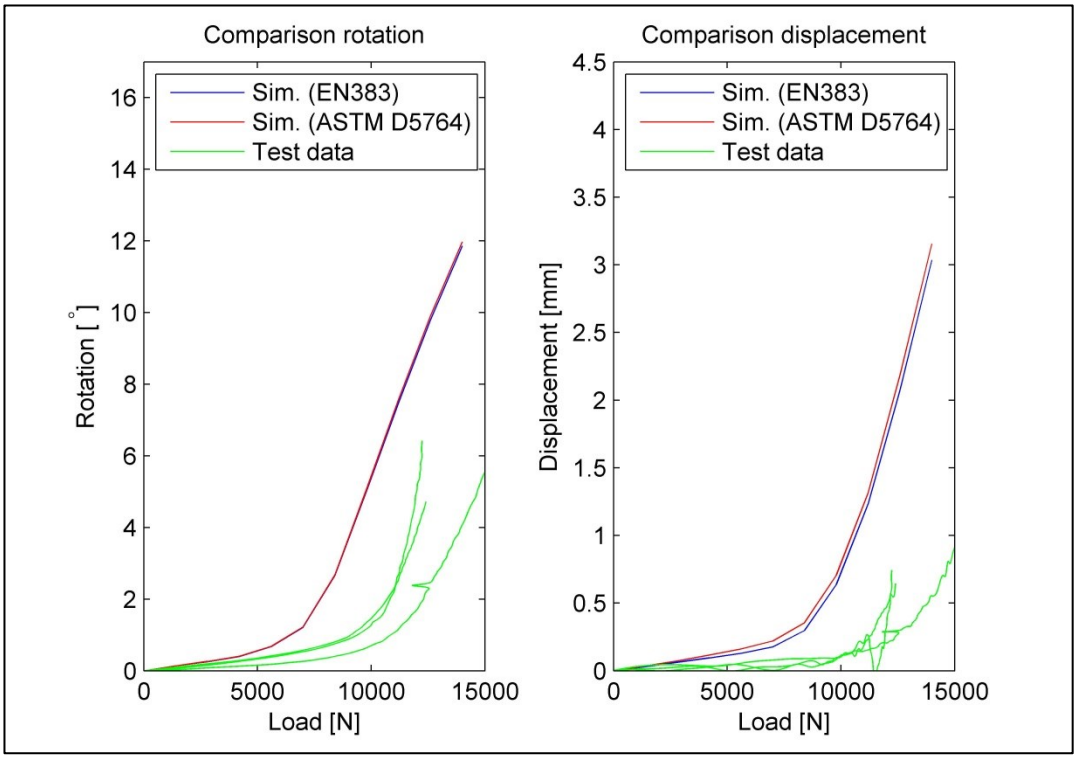

Figure 5-13: Comparison Simulation data and Test results for mean density – uncalibrated

A closer examination of the embedment strength tests performed in Chapter 4 and the tests on a fastener-group performed in this Chapter, revealed one significant difference. In the embedment-strength tests all of the wood-chips created while inserting the bolts fell out of the hole! This resulted in a loose fit of the bolt in a now oversized hole. In the real world application of this type of self-tapping fastener, the wood chips act as "filler" causing the bolt to fit very tightly in its hole.

Figure 5-14: Matrix of burned wood chips

Figure 5-15: Measurement of the matrix-thickness

Two assumptions were made to explain the tight fit:

1. **The compressed "filler" material surrounding the bolt will cause 100% of the bolt's diameter to bear loads**

Typically, only about 60% [9] of the bolt's diameter acts as direct bearing with the other 40% the wood being pushed aside causing splitting forces. In the case of the self-tapping bolts, the filler-matrix is compressed and heated because of the drilling process. This denser material with its exact fit to the bolt results in a greater friction causing the entire bolt to bear the loads. As a result, the load in the LDD surfaces can be multiplied by a factor α_m of approximately 1.6.

2. **The tight fit will raise the initial stiffness**

In the case of an oversized hole, the bolt theoretically touches the surface of the hole in a very small area; it requires a small amount of displacement and deformation of the wood to get in touch on the full diameter. During this process, there are small deformations with insignificant forces that lead to an initial minimal stiffness. However, with the surrounding tight fitting matrix the self-tapping bolts are in contact with the entire diameter from the very beginning. Lowering the displacement of the EN 383 LDD surface by an assumed initial deformation of Δx_{ini} = 0.1 mm (*0.004 inch*) demonstrated good results especially in the comparison of relatively small vertical displacement at lower loads.

The calibrated model is now in close accordance with the actual tests (Figure 5-16).

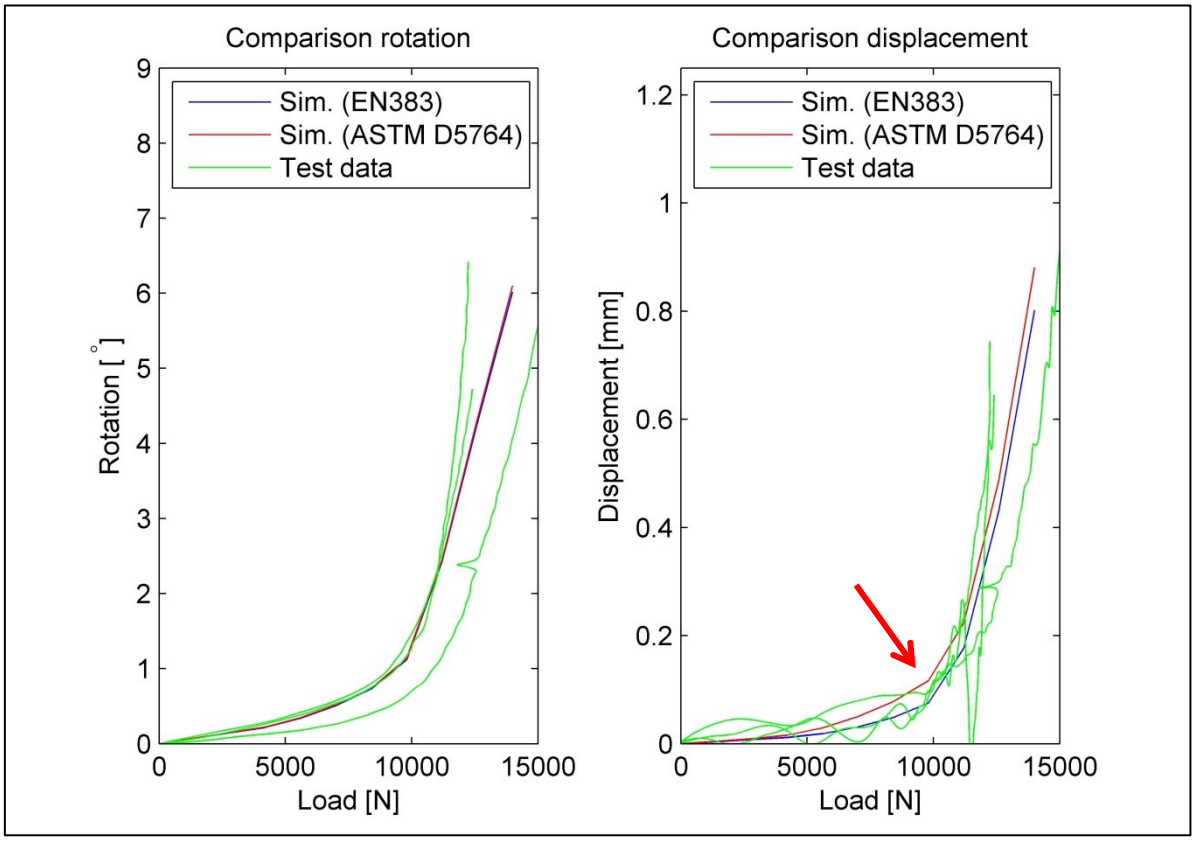

Figure 5-16: Comparison Simulation data and Test results for mean density – calibrated

The difference between EN 383 and ASTM D 5764 simulations can be explained by different measurement methods. In the ASTM method, the crosshead movement is measured. A slight amount of the measured displacement is due to the elasticity of the loaded part of the specimen; however, the minimal difference is discernable when stiffness is calculated (red arrow, Figure 5-16).

5.5 Comparison

When comparing the simulation and the calculated values based on the K_{ser} value (Chapter 1), the described lack of information in the approach with K_{ser} is clearly demonstrated (Figure 5-17); the plastic behavior cannot be reproduced.

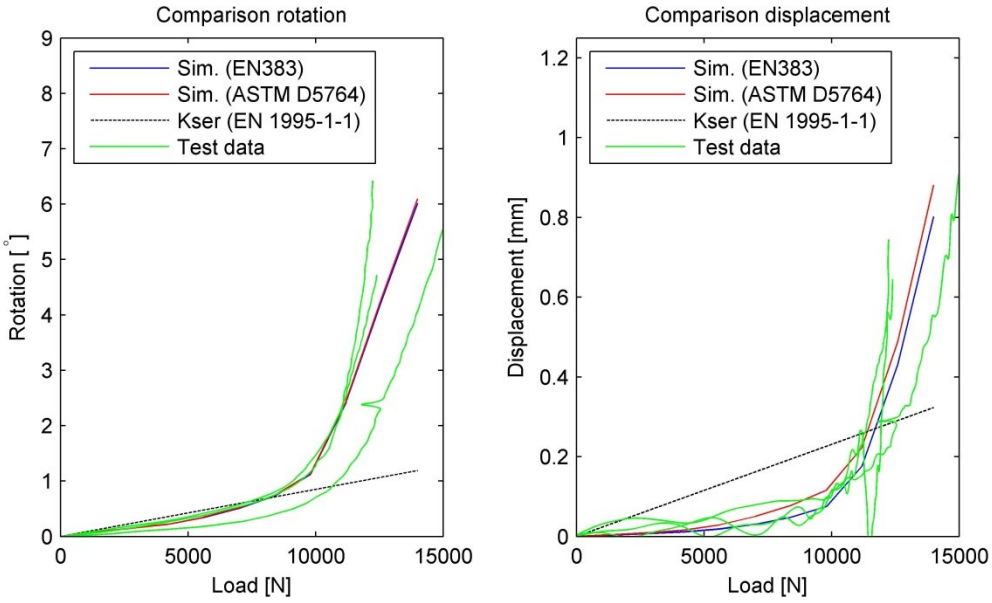

Figure 5-17: Comparison of test data, simulation and approach with K_{ser}

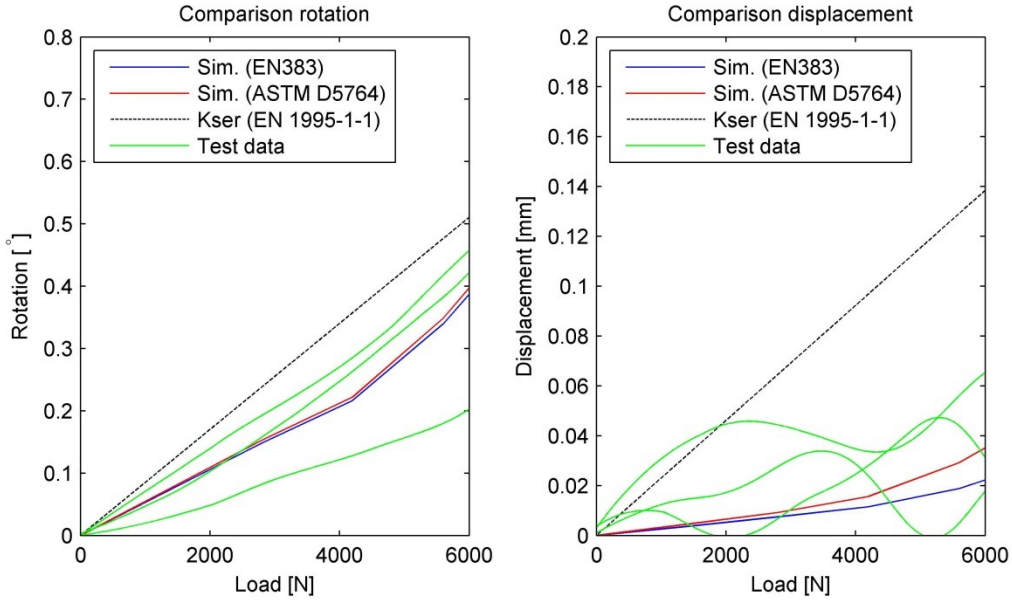

Figure 5-18: Comparison of test data, simulation and approach with K_{ser} zoom allowable load-range

The European building-code's allowable load for this connection is approximately 5'000 N (*1'124 lb.*). Beneath this limit, the connection demonstrates an almost linear stiffness; however the approach with K_{ser} does not represent the average of the test data; it underestimates the stiffness and consequently overestimates the deformations.

Conclusion

The definition of bearing strength values is of significant importance in timber construction. Both of the codes, European and American represent effective frameworks for gathering consistent and comparable values. As there is a large variety of fasteners with different diameters and multiple timber products, it is understandable that the codes sometimes are pushed to their limits.

The ASTM D 5764 procedure is simple and easy to use; the constant load pattern and the measurement of crosshead movement is uncomplicated to set up and working with the data is straightforward.

Alternatively, the EN 383 is more complicated. Not only is the load pattern with its unloading and reloading cycle more difficult to precisely set, but the measurement of the deformations at the prescribed points is complex. Examining small diameter bolts requires relatively small specimen dimensions, which can then interfere with the larger LVDT dimensions. Due to the position of the measurement points, it is necessary to use a minimum of two measuring instruments, in order to eliminate the inevitable rotations. As the number of specimens increase, the complexity of the measurement setup becomes an issue.

The author suggests an alternative method to record the displacement by using a high-resolution digital camera equipped with a macro lens. This method would allow the measurement of displacements as well as rotations by using photogrammetric methods.

The EN 383 procedure might be more complex, but it is superior when the scope of the design includes stiffness calculations as well as bearing strength calculations. Especially if self-tapping bolts are used and a full-hole setup is required; in these instances the measured relative displacement between bolt and hole reflected by the European code is more accurate.

A problem both codes share is that they are not accurate for the reviewed self-tapping bolts. The result of the inaccuracy is the matrix of burned and compacted woodchips surrounding the bolt that was created while placing the fastener. This matrix is a layer of a hard, plastic-like material, containing steel shavings located at the adjacency of the bolt and the steel plate and can be best described as a “footing” for the bolt in the borehole.

To accommodate this behavior in the simulation, the results from the two testing codes must be modified.

- Bearing strength must be multiplied by a factor α_m of 1.6
- Displacements must be reduced by a factor Δx_{ini} of 0.1 mm (*0.004 inch*)

Another way to take this effect into account would be trying to produce specimens with the described matrix in place for the embedment tests according to EN 383 respectively ASTM D 5764. This would be a challenging effort.

The approach with the K_{ser} value proposed in the EN 1995-1-1 is straightforward and easy to use. However, the predicted stiffness is inadequate in the case of self-tapping bolts. Both, over and underestimation can be problematic in construction. An overestimated stiffness might result in lower deformations than expected; an underestimated stiffness might lead to higher loads than expected.

Further research should be done relating to the stiffness of self-tapping bolt connections. Additional tests with both EN 383 and ASTM D 5764 procedures should be carried out with the results collected in a LDD surface databank. Carrying out tests on connections and comparing the results with simulations would allow for a more accurate definition of the two applied modification factors α_m and Δx_{ini}.

As in real world applications most likely the force is applied in a random angle, these tests should not only be carried out parallel and perpendicular to grain, but also in different angles like 15°, 30° and 45°.

Bibliography

[1] Rothoblaas, "Rothoblaas", [Online]. Available: http://www.rothoblaas.com/uploads/media/screws-for-wood-en.pdf. [Accessed 22 March 2016].

[2] H. J. Blass and T. Uibel, "Tragfähigkeit von Stiftförmigen Verbindungsmitteln in Brettsperrholz", vol. Karlsruher Berichte zum Ingenieurholzbau, no. 8, 2007.

[3] K. W. Johansen, "Theory of Timber Connections", *IABSE publications = Mémoires AIPC = IVBH Abhandlungen,* vol. 9, 1949.

[4] A. Meyer, "Die Tragfähigkeit von Nagelverbindungen bei statischer Belastung", *Holz als Roh- und Werkstoff,* no. 15, pp. 96-109, February 1957.

[5] Austrian Standards Institute, *Timber Structures — Test Methods — Determination of Embedment Strength and Foundation Values for Dowel Type Fasteners,* Austrian Standards Institute, 2007.

[6] American Society for Testing and Materials, *Standard Test Method for Evaluating Dowel-Bearing Strength of Wood and Wood-Based Products,* American Society for Testing and Materials, 2007.

[7] Austrian Standards Institute, *Eurocode 5: Design of Timber Structures,* Austrian Standards Institute, 2015.

[8] I. Gavric, "Seismic Behaviour of Cross-Laminated Timber Buildings," 2013. [Online]. Available: http://hdl.handle.net/10077/8638.

[9] G. Hochreiner and T. K. Bader, "Stiftförmige Verbindungsmittel im EC5 und baustatische Modellbildung mittels kommerzieller Statiksoftware", *Bauingenieur,* no. 88, p. 275–289, January 2013.

[10] American Wood Council, *NDS National Design Specification for Wood Construction,* American Wood Council, 2015.

[11] Austrian Standards Institute, *Timber Structures - Test Methods - Determination of the Yield Moment of Dowel Type Fasteners,* Austrian Standards Institute, 2009.

[12] Austrian Standards Institute,
Timber Structures - Test Methods - Load Bearing Nails, Screws, Dowels and Bolts,
Austrian Standards Institute, 2009.

[13] United States Geoscience and Environmental Change Science Center (USGS), "USGS",
[Online]. Available: http://gec.cr.usgs.gov/data/little/fraxamer.pdf.
[Accessed 01 July 2016].

[14] United States Geoscience and Environmental Change Science Center (USGS), "USGS",
[Online]. Available: http://gec.cr.usgs.gov/data/little/picemari.pdf.
[Accessed 01 July 2016].

[15] Nordic, "Nordic," [Online]. Available: http://nordic.ca/data/files/datasheet/file/T-S01_ePropertiesNordicLam.pdf.
[Accessed 11 March 2016].

[16] Austrian Standards Institute,
Wood-Based Panels – Determination of Moisture Content, 2005-12-01 ed., Austrian Standards Institute, 2005.

Appendix

Load - displacement curves for Single Bolt – embedment testing:

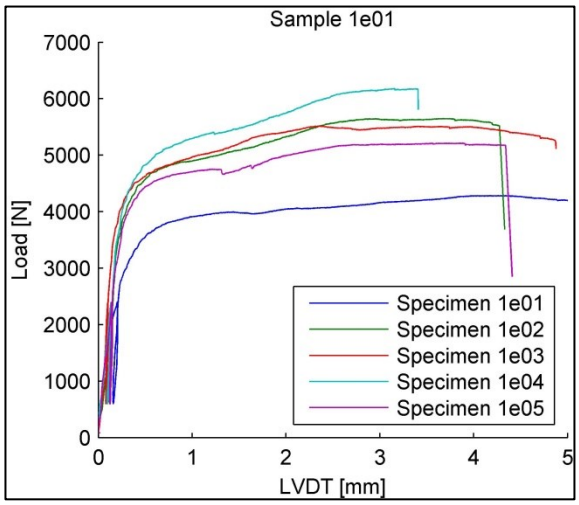

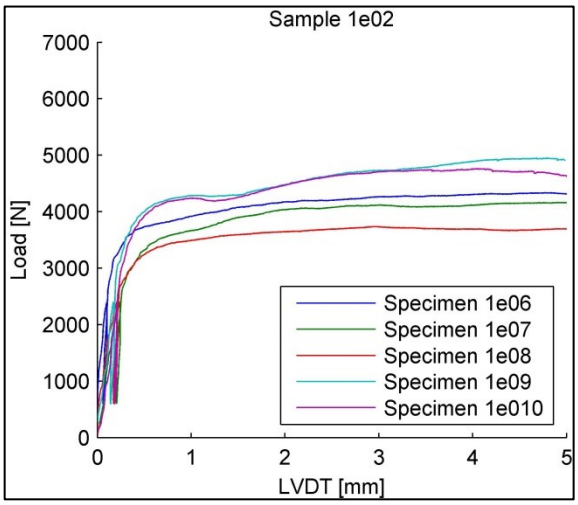

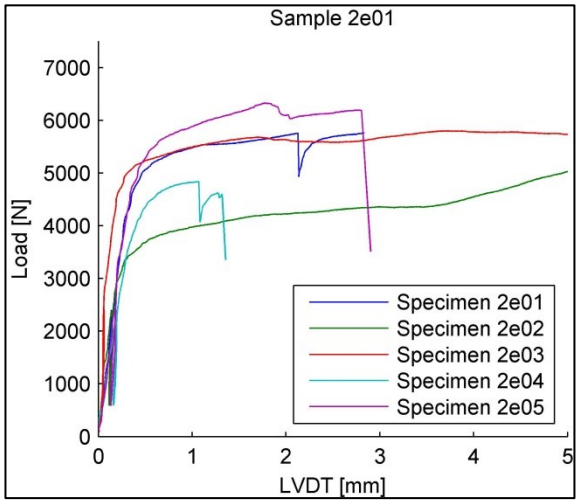

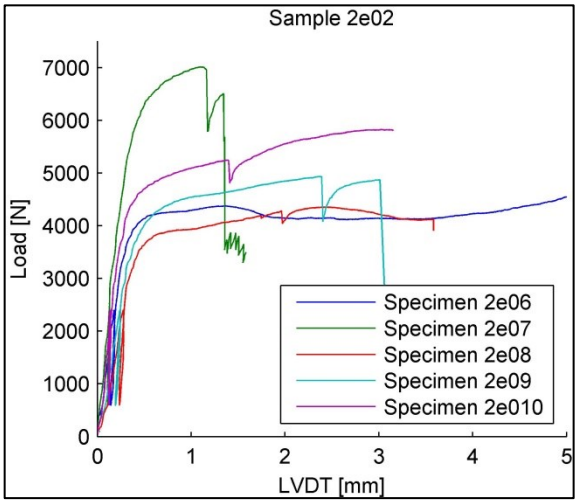

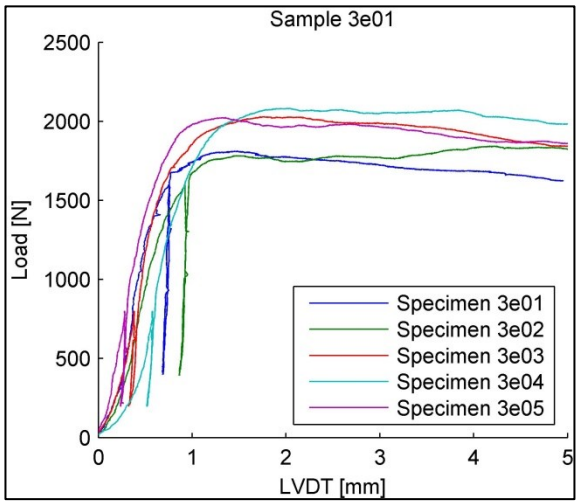

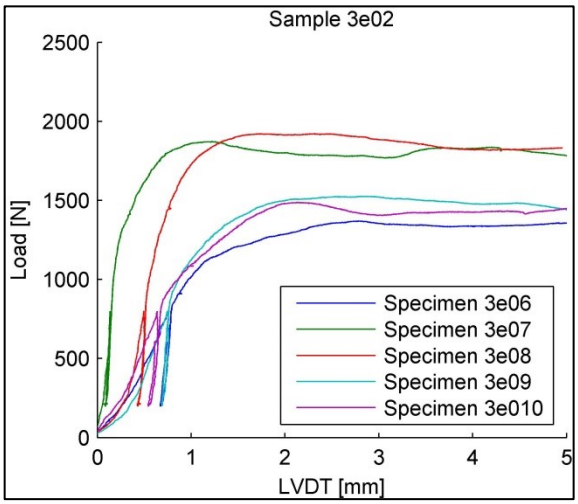

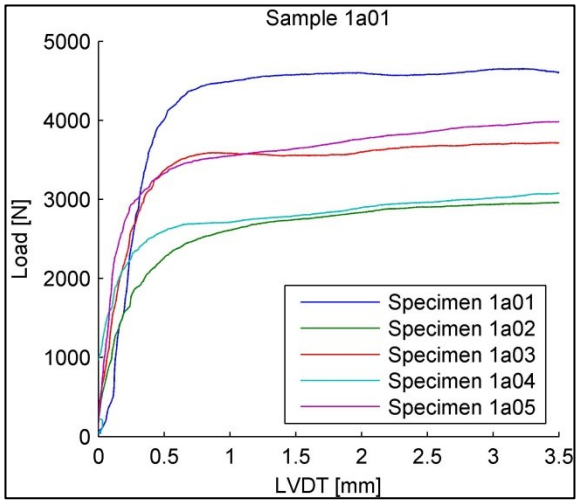
Sample 1a01
Load [N]
LVDT [mm]
Specimen 1a01
Specimen 1a02
Specimen 1a03
Specimen 1a04
Specimen 1a05

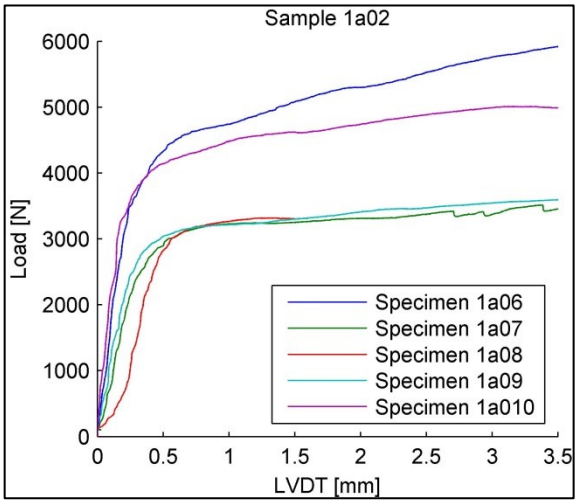
Sample 1a02
Load [N]
LVDT [mm]
Specimen 1a06
Specimen 1a07
Specimen 1a08
Specimen 1a09
Specimen 1a010

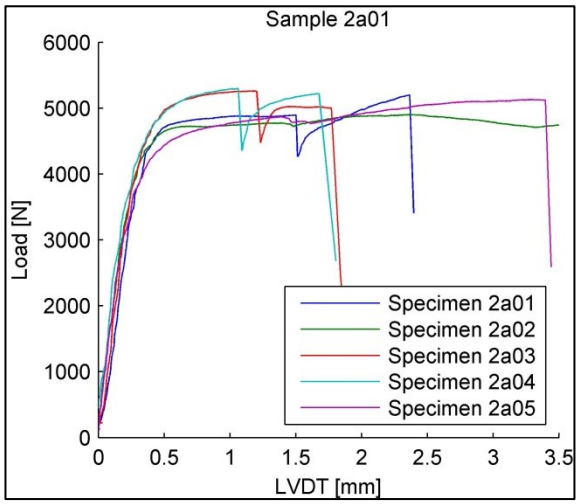
Sample 2a01
Load [N]
LVDT [mm]
Specimen 2a01
Specimen 2a02
Specimen 2a03
Specimen 2a04
Specimen 2a05

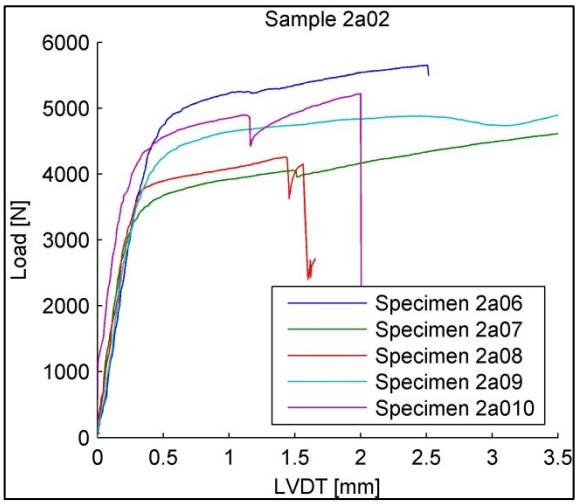
Sample 2a02
Load [N]
LVDT [mm]
Specimen 2a06
Specimen 2a07
Specimen 2a08
Specimen 2a09
Specimen 2a010

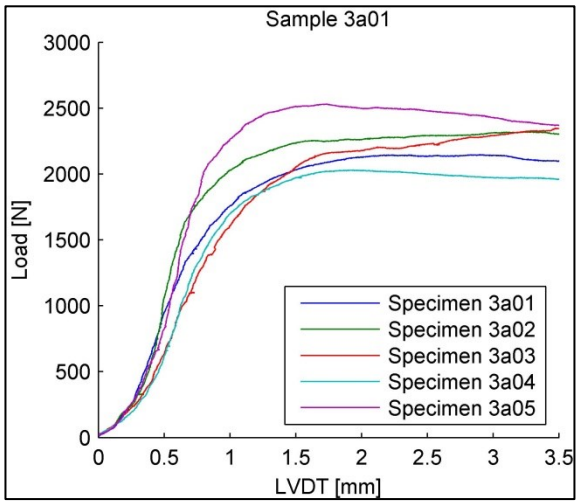
Sample 3a01
Load [N]
LVDT [mm]
Specimen 3a01
Specimen 3a02
Specimen 3a03
Specimen 3a04
Specimen 3a05

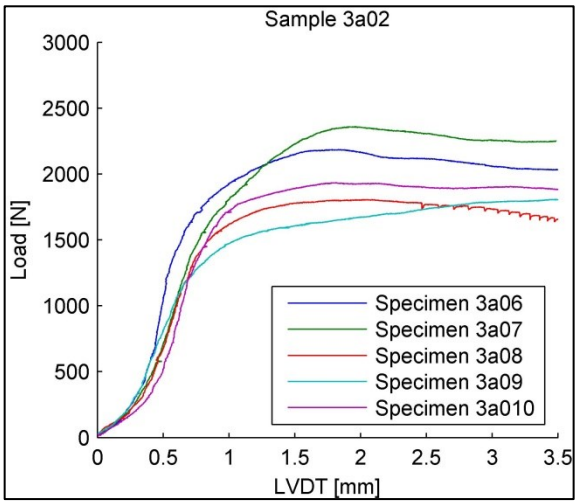
Sample 3a02
Load [N]
LVDT [mm]
Specimen 3a06
Specimen 3a07
Specimen 3a08
Specimen 3a09
Specimen 3a010

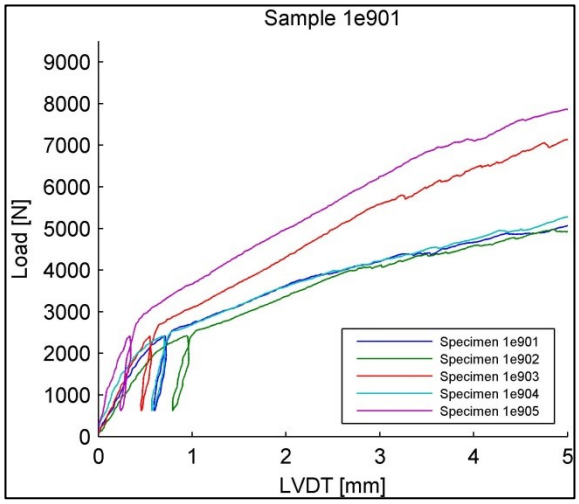
Sample 1e901
Load [N]
LVDT [mm]
Specimen 1e901
Specimen 1e902
Specimen 1e903
Specimen 1e904
Specimen 1e905

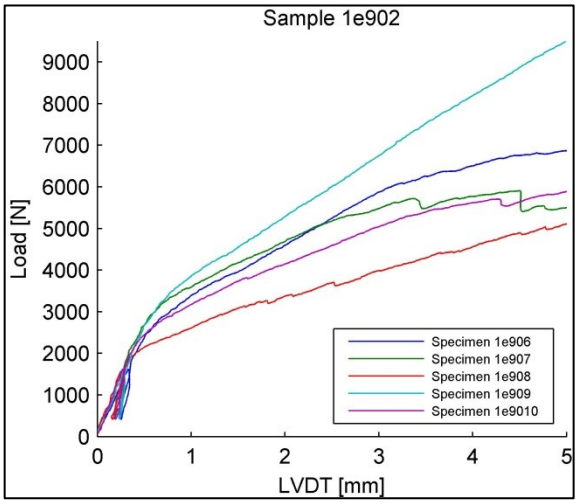
Sample 1e902
Load [N]
LVDT [mm]
Specimen 1e906
Specimen 1e907
Specimen 1e908
Specimen 1e909
Specimen 1e9010

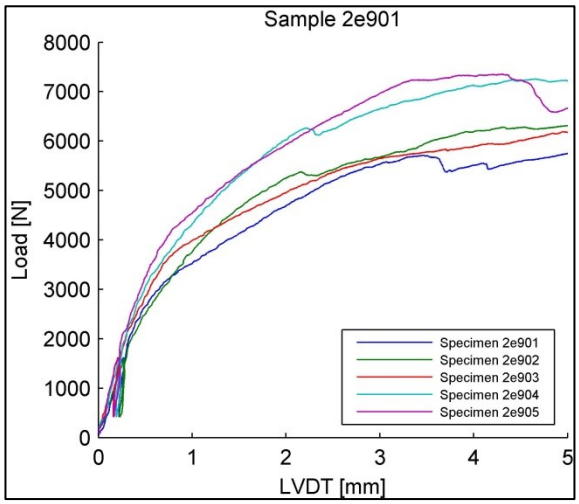
Sample 2e901
Load [N]
LVDT [mm]
Specimen 2e901
Specimen 2e902
Specimen 2e903
Specimen 2e904
Specimen 2e905

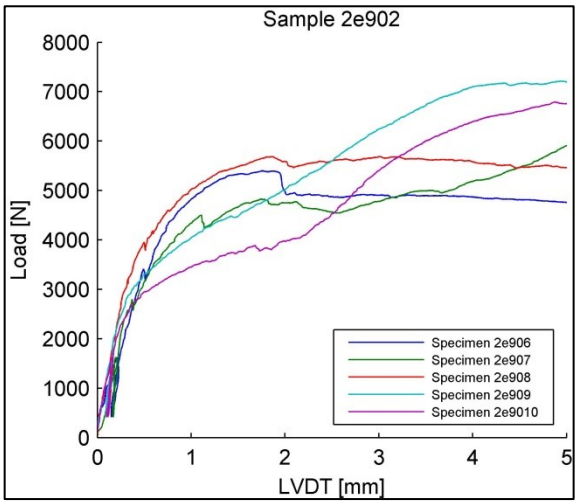
Sample 2e902
Load [N]
LVDT [mm]
Specimen 2e906
Specimen 2e907
Specimen 2e908
Specimen 2e909
Specimen 2e9010

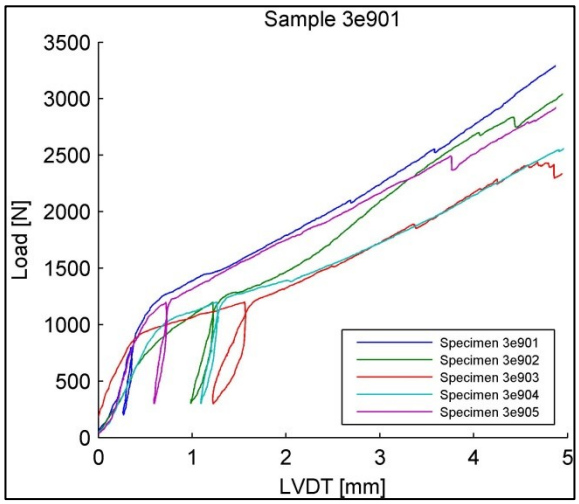
Sample 3e901
Load [N]
LVDT [mm]
Specimen 3e901
Specimen 3e902
Specimen 3e903
Specimen 3e904
Specimen 3e905

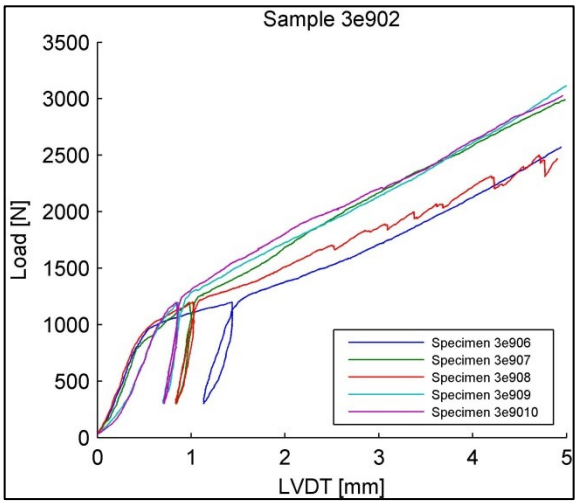
Sample 3e902
Load [N]
LVDT [mm]
Specimen 3e906
Specimen 3e907
Specimen 3e908
Specimen 3e909
Specimen 3e9010

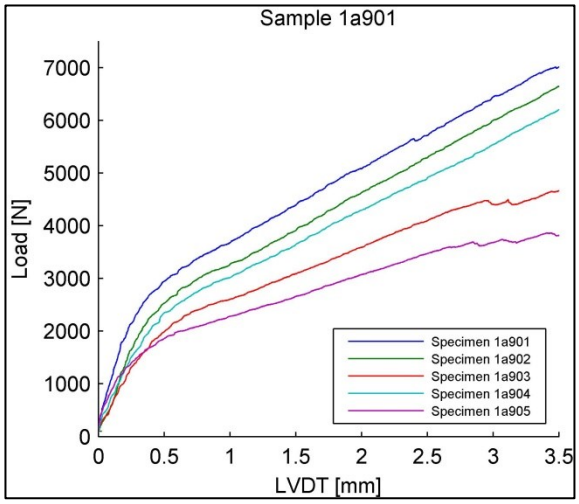
Sample 1a901
Load [N]
LVDT [mm]
Specimen 1a901
Specimen 1a902
Specimen 1a903
Specimen 1a904
Specimen 1a905

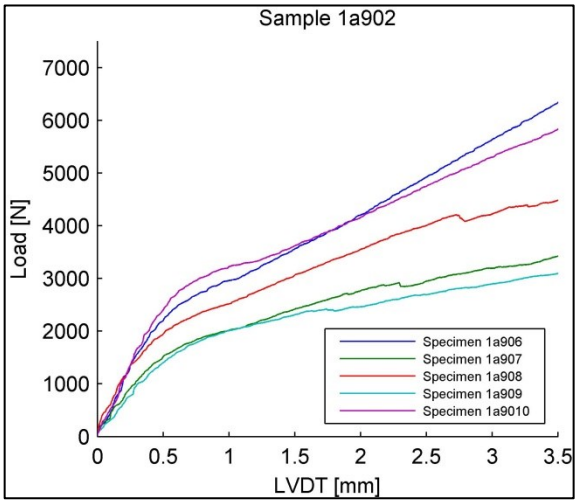
Sample 1a902
Load [N]
LVDT [mm]
Specimen 1a906
Specimen 1a907
Specimen 1a908
Specimen 1a909
Specimen 1a9010

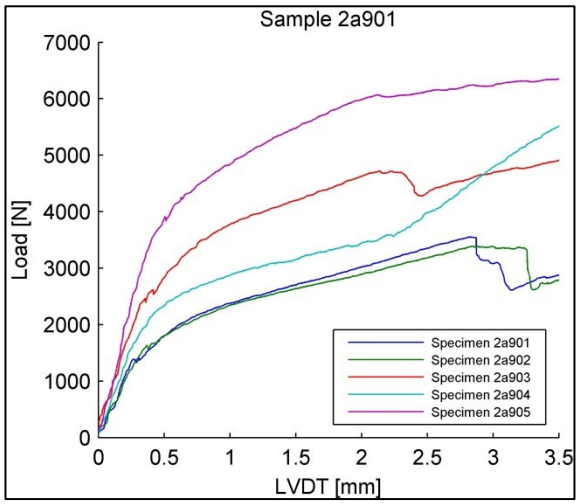
Sample 2a901
Load [N]
LVDT [mm]
Specimen 2a901
Specimen 2a902
Specimen 2a903
Specimen 2a904
Specimen 2a905

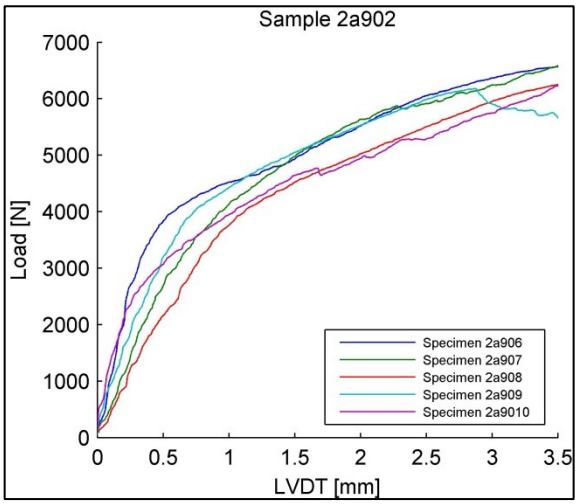
Sample 2a902
Load [N]
LVDT [mm]
Specimen 2a906
Specimen 2a907
Specimen 2a908
Specimen 2a909
Specimen 2a9010

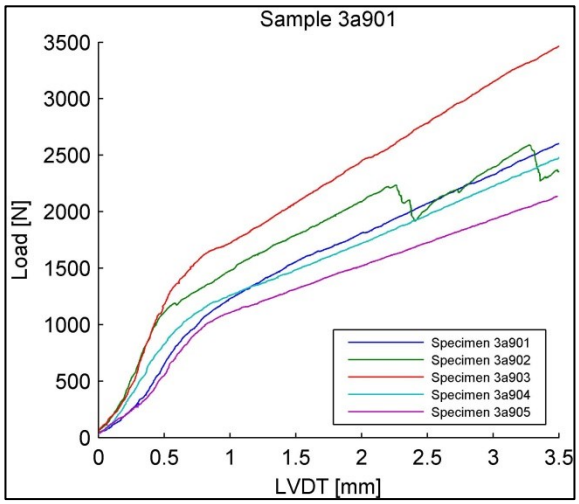
Sample 3a901
Load [N]
LVDT [mm]
Specimen 3a901
Specimen 3a902
Specimen 3a903
Specimen 3a904
Specimen 3a905

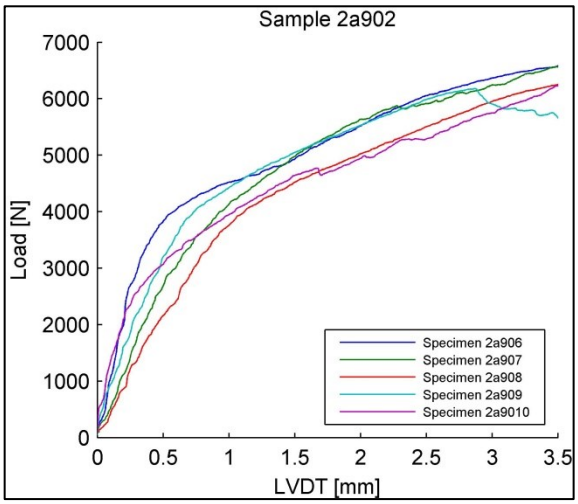
Sample 2a902
Load [N]
LVDT [mm]
Specimen 2a906
Specimen 2a907
Specimen 2a908
Specimen 2a909
Specimen 2a9010

Verpflichtungs- und Einverständniserklärung

Ich erkläre, dass ich meine Masterarbeit selbstständig verfasst und alle in ihr verwendeten Unterlagen, Hilfsmittel und die zugrunde gelegte Literatur genannt habe.

Ich nehme zur Kenntnis, dass auch bei auszugsweiser Veröffentlichung meiner Masterarbeit die Universität, das/die Institut/e und der/die Arbeitsbereich/e, an dem/denen die Masterarbeit ausgearbeitet wurde, und die Betreuerin/nen bzw. der/die Betreuer zu nennen sind.

Ich nehme zur Kenntnis, dass meine Masterarbeit zur internen Dokumentation und Archivierung sowie zur Abgleichung mit der Plagiatssoftware elektronisch im Dateiformat pdf/A ohne Kennwortschutz bei der/dem Betreuerin/Betreuer einzureichen ist, wobei auf die elektronisch archivierte Masterarbeit nur die/der Betreuerin/Betreuer der Masterarbeit und das studienrechtliche Organ Zugriff haben.

Innsbruck, am 13.10.2016 ……

Dominik WINKLER